UNIVERSITATEA DE MEDICINĂ ȘI FARMACIE „CAROL DAVILA”, BUCUREȘTI

ȘCOALA DOCTORALĂ DOMENIUL MEDICINĂ

EFICIENȚA TERAPIILOR MODERNE ÎN AMILOIDOZA CARDIACĂ: ROLUL IMAGISTICII MULTIMODALE

REZUMAT AL TEZEI DE DOCTORAT REDACTAT ÎN LIMBA ENGLEZĂ

Coordonator de doctorat:

PROF. UNIV. DR. RUXANDRA OANA JURCUȚ

Student – doctorand:

DR. GABRIELA NECULAE

2026

SUMMARY

SECTION I: CURRENT KNOWLEDGE ON THE DISEASE 3

1.Introduction and Objectives of the Thesis 3

2. Pathophysiology 4

3. Clinical Aspects 5

4. Diagnostic Approach in Cardiac Amyloidosis 7

5. Staging and Prognosis 10

6. Management 10

SECTION II: PERSONAL CONTRIBUTIONS TO THE FIELD 13

1. Dynamic Assessment of Cardiac Involvement in ATTR Amyloidosis: From Prognosis to Disease Progression 13

Study 1: ATTR Variants In Eastern And Western Europe: A Phenotypic Comparison Of Romanian And French ATTRv Cohorts 13

Discussion points 16

Study 2. A New Staging System for Hereditary ATTR in the Era of Specific Therapies 17

Discussion points 21

Study 3: Serial Multimodality Imaging Demonstrates Disease Stability In Transthyretin Cardiac Amyloidosis Receiving Contemporary Disease-Modifying Therapies 23

Discussion points 26

2. Dynamic Assessment of Cardiac Involvement in Light-Chain Amyloidosis: From Prognosis to Organ Response 27

Study 1. Incorporating Right Ventricular Function into the European Modified Mayo Staging System 27

Discussion points 31

Study 2. Beyond Biomarker Response: Multimodality Imaging Evidence Of Cardiac Response After Daratumumab-Based Therapy In AL Amyloidosis 32

Discussion points 36

Section II Synthesis: Results-Based Contribution 37

FINAL CONSIDERATIONS 38

BIBLIOGRAPHY 39

SECTION I: CURRENT KNOWLEDGE ON THE DISEASE

1. Introduction and Objectives of the Thesis

Systemic amyloidosis comprises a heterogeneous group of disorders characterized by extracellular deposition of misfolded proteins in the form of insoluble amyloid fibrils. These fibrils are composed of low-molecular-weight protein subunits arranged in a characteristic cross beta-sheet configuration, which explains their structural stability and resistance to proteolytic degradation [1]. Amyloid deposits also contain non-fibrillar components, including serum amyloid P component and glycosaminoglycans, which further stabilize aggregates and contribute to their persistence in tissues [2]. Cardiac involvement is one of the most severe forms of organ damage because it directly determines functional limitation, treatment tolerance, prognosis, and survival. The thesis focuses primarily on the two most frequent forms of cardiac amyloidosis: light-chain amyloidosis and transthyretin amyloidosis [2,3].

Cardiac amyloidosis has long been considered rare and underdiagnosed, but its real prevalence has become increasingly apparent with improved clinical awareness and the introduction of non-invasive diagnostic algorithms. ATTR cardiomyopathy is now recognized among elderly patients with unexplained heart failure with preserved ejection fraction, left ventricular hypertrophy, or severe aortic stenosis referred for transcatheter valve intervention [4]. Despite this progress, delayed diagnosis remains common and has major prognostic consequences, especially in AL amyloidosis, where advanced cardiac involvement is associated with early mortality. The development of modern therapies has changed the field: plasma cell-directed treatment has improved outcomes in AL amyloidosis [5,6], while transthyretin stabilizers, gene silencers, and emerging amyloid-depleting or gene-editing strategies have transformed ATTR amyloidosis into a chronic disease requiring longitudinal monitoring [7,8].

The overarching aim of the thesis is to investigate the evolving role of multimodality cardiac assessment in amyloidosis, with emphasis on risk stratification, disease progression, and treatment response in the era of disease-modifying therapies. The specific objectives are to synthesize current knowledge regarding AL and ATTR amyloidosis; to clarify diagnostic, staging, and therapeutic pathways; to evaluate echocardiography, cardiac magnetic resonance, and nuclear imaging in diagnosis and follow-up; to describe the heterogeneity of hereditary ATTR populations; to test improved prognostic approaches that integrate biomarkers and imaging; and to explore whether serial imaging can distinguish disease progression, stabilization, or recovery during treatment.

2. Pathophysiology

Amyloid deposition is presented in the thesis as a dynamic biological process rather than as a passive accumulation of insoluble material. Under physiological conditions, protein homeostasis is maintained by coordinated mechanisms that ensure correct folding, degradation, and elimination of misfolded proteins [16]. In amyloidosis, this balance is disrupted by increased precursor production, genetic instability of the precursor protein, impaired clearance, or progressive amplification of fibril formation. Clearance mechanisms include enzymatic degradation, phagocytic uptake by innate immune cells, and transport-mediated removal, but these mechanisms are often insufficient, particularly with aging and declining proteostatic capacity [17–19].

A key concept is amyloid "seeding." Once fibrils are formed, they may act as templates that recruit native protein molecules and promote conversion into misfolded conformations. Experimental studies have shown that transthyretin fibrils extracted from patients can accelerate fibrillogenesis of both mutant and wild-type transthyretin under physiological conditions [20,21]. This mechanism helps explain why amyloid diseases may accelerate over time and why deposition may persist even when circulating precursor protein concentrations are reduced by therapy.

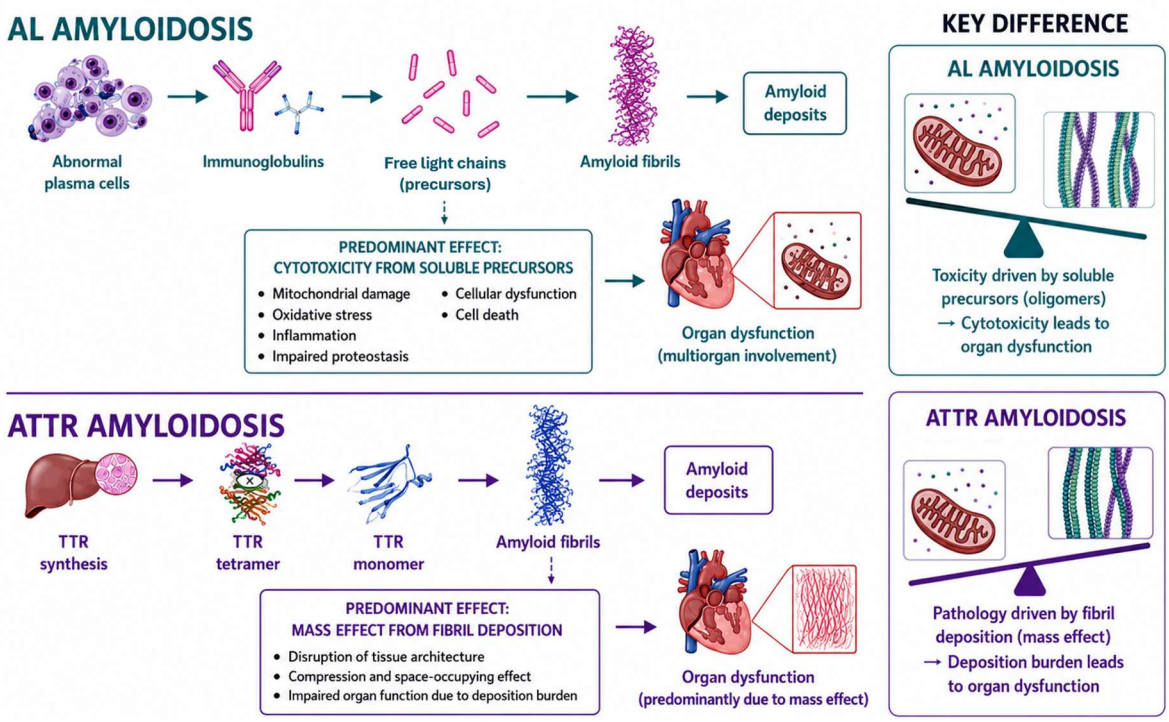


Figure 1. Pathophysiological Differences in Cardiac AL and ATTR Amyloidosis. Schematic representation of the main pathophysiological determinants of cardiac damage and cardiac dysfunction in light chains (AL) and ATTR amyloidosis

Although AL and ATTR amyloidosis converge on the final pathway of extracellular fibril deposition, their pathophysiological mechanisms differ substantially. AL amyloidosis originates from a clonal plasma cell disorder that produces unstable immunoglobulin light chains [22,23]. These light chains aggregate into amyloid fibrils but also exert direct cardiotoxic effects, including oxidative stress and cellular injury, which explains the rapid progression and severe heart failure often seen in AL cardiomyopathy even at lower degrees of amyloid burden [24]. In contrast, ATTR amyloidosis results from destabilization of the transthyretin tetramer, dissociation into monomers, misfolding, and aggregation. This may occur as an age-related process in ATTRwt or be accelerated by pathogenic TTR mutations in ATTRv [2].

The thesis places special emphasis on the heterogeneity of hereditary ATTR. More than 130 pathogenic TTR variants have been described, generating neurologic, cardiac, or mixed phenotypes [25,26]. Val30Met is the most common variant worldwide, with early-onset neurologic disease in endemic regions such as Portugal, Scandinavia, and Japan, but later-onset and more cardiac expression in non-endemic areas. Val122Ile is frequent in the United States and produces a late-onset cardiac phenotype with incomplete penetrance [25,26]. Romania represents a distinct ATTRv population, characterized by geographical clustering and predominance of Glu54Gln, associated with early onset and mixed neurologic and cardiac involvement [27]. This genotype-dependent heterogeneity supports the thesis rationale for refined, population-sensitive risk stratification.

3. Clinical Aspects

Systemic amyloidoses are multisystem diseases with highly heterogeneous and often nonspecific clinical presentations. Because early symptoms are frequently subtle, diagnosis is commonly delayed until organ dysfunction is established [28]. Cardiac involvement is the major prognostic determinant in both AL and ATTR amyloidosis, but isolated cardiac disease is uncommon. Instead, cardiac manifestations often coexist with neurologic, autonomic, renal, gastrointestinal, musculoskeletal, or soft-tissue abnormalities [28,29]. Recognition of clustered “red flags” is therefore central to early suspicion and referral.

ATTR amyloidosis is frequently preceded by extracardiac manifestations such as bilateral carpal tunnel syndrome, lumbar spinal stenosis, spontaneous distal biceps tendon rupture, peripheral neuropathy, and autonomic dysfunction. These features may appear years before cardiac diagnosis. AL amyloidosis, in contrast, is more often suggested by nephrotic-range proteinuria, macroglossia, periorbital purpura, soft tissue involvement, and rapidly

progressive heart failure [31]. The thesis emphasizes that these manifestations should be interpreted collectively rather than as isolated findings.

Laboratory work-up has three major objectives: identifying the amyloid precursor protein, assessing organ involvement and disease severity, and establishing baseline values for staging and follow-up. The diagnostic sequence requires exclusion of AL amyloidosis using serum and urine immunofixation electrophoresis and serum free light-chain quantification before proceeding to non-invasive ATTR diagnosis by bone scintigraphy [31]. Once ATTR is confirmed, TTR genetic testing is mandatory to distinguish ATTRv from ATTRwt and to guide family screening. Cardiac biomarkers such as NT-proBNP and troponins support staging and prognosis, while creatinine, eGFR, proteinuria, liver tests, coagulation profile, and complete blood count help define systemic involvement and treatment risk.

In the heart, amyloid deposition expands the interstitial space, increases ventricular stiffness, impairs relaxation and filling, and reduces stroke volume and cardiac output. Early in the disease, ejection fraction may remain preserved, but longitudinal systolic function and stroke volume are often reduced. Clinically, this produces restrictive cardiomyopathy with heart failure, systemic congestion, low-output symptoms, conduction disturbances, and arrhythmias [24,30]. AL amyloidosis often produces rapidly progressive heart failure with higher biomarker levels because of both infiltration and direct light-chain toxicity, while ATTR cardiomyopathy usually progresses more slowly and is frequently associated with older age, atrial fibrillation, conduction disease, and low-flow physiology [32–36].

Neurologic involvement includes peripheral polyneuropathy and autonomic dysfunction. In hereditary ATTR, neuropathy varies according to genotype, ranging from frequent involvement in early-onset Val30Met to lower prevalence in Val122Ile [31,41,42]. Symptoms often begin as small-fiber neuropathy with burning pain, numbness, and impaired temperature sensation, followed by large-fiber involvement, weakness, gait disturbance, and eventual loss of ambulation. Autonomic dysfunction may manifest as orthostatic hypotension, digestive dysmotility, diarrhea or constipation, urinary retention, erectile dysfunction, and weight loss [28,41]. Diagnostic confirmation may require nerve conduction studies, electromyography, sudomotor testing, and structured neurologic scoring systems such as mNIS+7 [42–47].

Other extracardiac manifestations help differentiate amyloid subtypes. Gastrointestinal symptoms may result from autonomic dysfunction, mucosal amyloid infiltration, vascular involvement, malabsorption, or congestion [48,49]. Musculoskeletal manifestations are especially common in ATTR and may precede cardiac disease by 5–10 years; carpal tunnel

syndrome, trigger finger, lumbar spinal stenosis, rotator cuff pathology, and distal biceps tendon rupture are important clues [50–54]. Renal involvement is much more common in AL amyloidosis, often presenting with nephrotic syndrome and progressive renal dysfunction, whereas in ATTR cardiomyopathy renal impairment is usually related to cardiorenal syndrome and has prognostic relevance through eGFR-based staging [9,32].

4. Diagnostic Approach in Cardiac Amyloidosis

Diagnosis begins with clinical suspicion based on cardiac and extracardiac red flags. Initial evaluation integrates symptoms, electrocardiography, biomarkers, and echocardiography [32]. Patients may present with exertional dyspnea, fatigue, edema, reduced exercise capacity, palpitations, syncope, or low-output symptoms. Biomarkers often show disproportionately elevated NT-proBNP and mildly increased troponin relative to conventional imaging findings [3]. ECG findings may include low QRS voltages, a low voltage-to-mass ratio, pseudo-infarction pattern, atrioventricular or bundle branch block, bradyarrhythmias, and atrial fibrillation [37–39]. These findings are not sufficiently sensitive alone but are highly suggestive when combined with unexplained left ventricular wall thickening.

Echocardiography remains the principal first-line imaging method for diagnosis and follow-up [3,31,55]. Typical findings include unexplained left ventricular hypertrophy, usually using a 12 mm threshold in the appropriate clinical context, reduced ventricular cavity size, biatrial enlargement, thickened valves, interatrial septal thickening, right ventricular wall thickening, pericardial effusion, advanced diastolic dysfunction, and restrictive filling [32,40]. Longitudinal systolic dysfunction may occur despite preserved ejection fraction, and relative apical sparing on strain imaging is a characteristic pattern. Current approaches also use multiparametric echocardiographic scores combining wall thickness, E/e′, TAPSE, GLS, and apical-to-basal strain ratios to improve diagnostic suspicion [3,57].

Cardiac magnetic resonance provides high-resolution assessment of cardiac structure, function, and tissue composition. Classic findings include diffuse subendocardial or transmural late gadolinium enhancement, abnormal myocardial nulling, elevated native T1, and markedly increased extracellular volume fraction [12,58–60]. ECV is particularly valuable because amyloid is deposited in the interstitial space; values may exceed 50%, higher than in many other causes of hypertrophy or fibrosis [58,60]. Native T1 may also be elevated, though it reflects amyloid, fibrosis, and edema. CMR is highly useful in differential diagnosis and for excluding

amyloidosis in selected cases, but it cannot by itself confirm amyloid type or reliably distinguish AL from ATTR cardiomyopathy [31,63].

The integrated diagnostic pathway requires immediate differentiation between AL and ATTR because treatment implications are urgent and fundamentally different. The first decisive step is screening for monoclonal protein with serum and urine immunofixation and serum free light-chain measurement [22,31,64]. If monoclonal studies are positive, AL amyloidosis must be considered, but tissue confirmation is required because monoclonal gammopathy may coexist with ATTR, especially in older patients [3,31,56]. Biopsy can be performed from involved organs or surrogate sites such as abdominal fat pad, bone marrow, or minor salivary glands, followed by amyloid typing using immunohistochemistry, immunoelectron microscopy, or preferably mass spectrometry [65–67].

If monoclonal studies are negative, bone-avid tracer scintigraphy becomes central for ATTR diagnosis. The most commonly used tracers are 99mTc-DPD, 99mTc-PYP, and 99mTc-HMDP [68]. Imaging protocols combine planar imaging with SPECT to confirm true myocardial uptake rather than blood-pool activity or extracardiac overlap [63,69]. The Perugini visual score grades myocardial uptake from 0 to 3. In the absence of a monoclonal protein, grade 2 or 3 uptake is highly specific and sufficient for a non-invasive diagnosis of ATTR cardiomyopathy [70]. TTR genetic testing is then required to distinguish hereditary from wild-type ATTR and to enable family counseling.

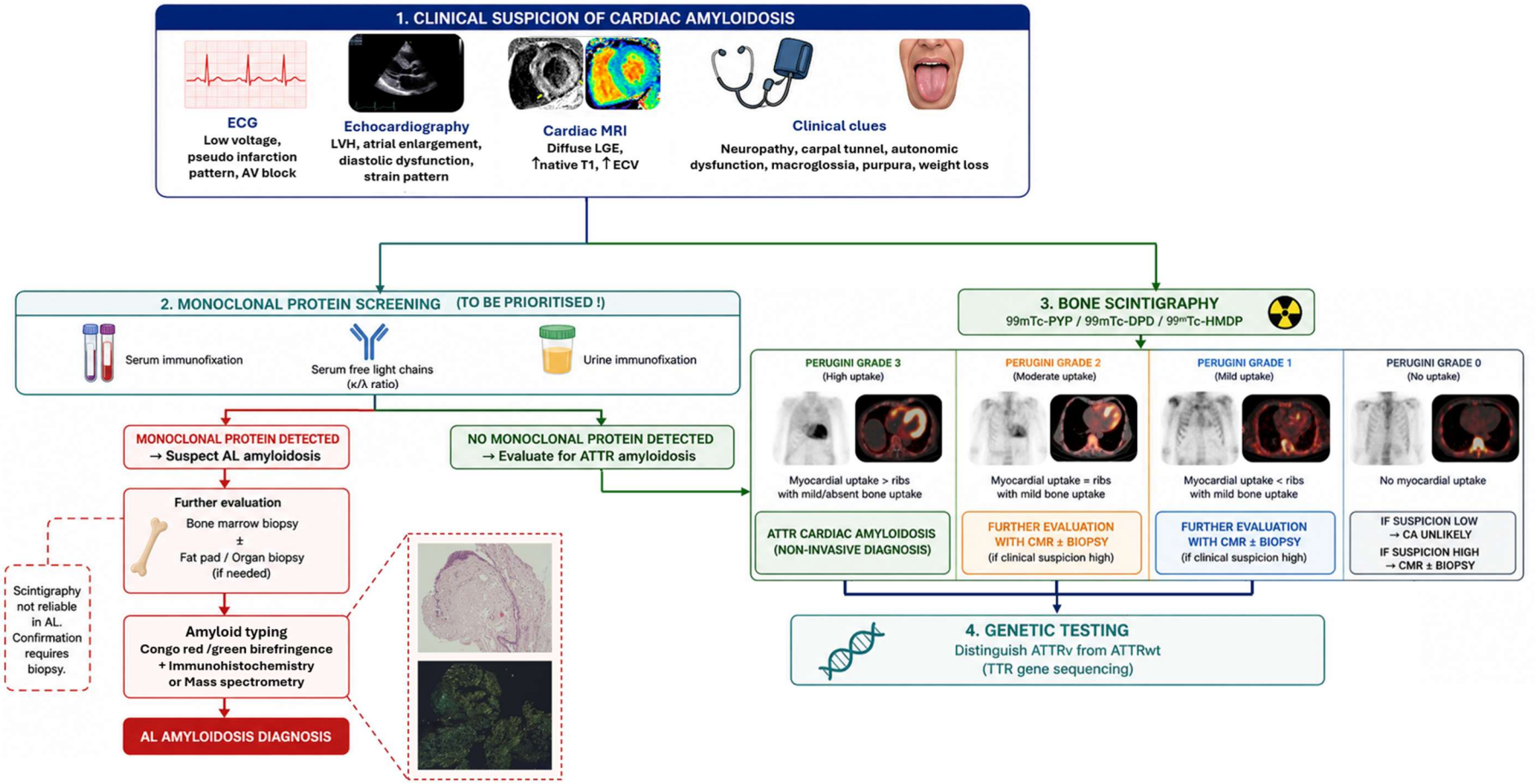


Figure 2. Contemporary diagnostic pathway for cardiac amyloidosis. Diagnostic workup begins with recognition of clinical and imaging red flags, followed by mandatory screening for a monoclonal protein. Positive monoclonal studies prompt evaluation for AL amyloidosis, whereas negative studies are followed by bone scintigraphy to identify ATTR cardiac amyloidosis. Tissue biopsy remains the reference standard when non-invasive testing is inconclusive. Genetic testing is subsequently performed in patients with ATTR amyloidosis to differentiate variant (ATTRv) from wild-type (ATTRwt) disease.

5. Staging and Prognosis

Staging in AL amyloidosis is primarily based on cardiac biomarkers and derives from Mayo Clinic models. The Mayo 2004 system used cardiac troponin T and NT-proBNP thresholds to classify patients into three stages [71]. The European modification subdivided stage III using an NT-proBNP threshold of 8500 ng/L, identifying stage IIIB patients with particularly poor short-term prognosis [72]. The revised Mayo 2012 model added the difference between involved and uninvolved free light chains, reflecting both cardiac damage and clonal burden [10,33]. Although these models remain fundamental, their discriminatory performance may be limited in advanced cardiac disease, leading to newer approaches such as the Mondor Amyloidosis Cardiac Staging system, which incorporates conjugated bilirubin as a marker of systemic congestion and end-organ dysfunction [73,74].

ATTR staging systems are also biomarker based. The Mayo ATTR model uses NT-proBNP and troponin T to stratify wild-type ATTR into three prognostic groups [11]. The National Amyloidosis Centre system combines NT-proBNP with estimated glomerular filtration rate and can be applied to both ATTRwt and ATTRv [9]. These systems remain useful for baseline risk stratification but have important limitations in the current era. They were developed largely in untreated populations and do not consistently integrate imaging markers, despite growing evidence that echocardiographic deformation and CMR tissue characterization carry prognostic and monitoring value [55,58–62]. This limitation provides the rationale for the thesis studies integrating GLS, CMR, and serial multimodality imaging into contemporary assessment.

6. Management

Management of AL amyloidosis is hematology-led and aims to suppress the plasma cell clone producing amyloidogenic light chains. Autologous stem cell transplantation with high-dose melphalan may provide durable responses but is suitable for only a minority of carefully selected patients because advanced cardiac involvement increases treatment-related risk [23,76]. In transplant-ineligible patients, outcomes have improved substantially with proteasome inhibitor-based therapy, especially bortezomib-cyclophosphamide-dexamethasone, and with monoclonal antibody therapy [5,75,77]. Daratumumab, an anti-CD38 antibody, combined with bortezomib, cyclophosphamide, and dexamethasone, has become a key first-

line regimen after demonstrating superior hematologic and organ responses in newly diagnosed AL amyloidosis [78].

Response assessment in AL amyloidosis includes hematologic response and organ response. Complete hematologic response requires absence of monoclonal protein on immunofixation and normalization or favorable shift of the free light-chain ratio [79]. The therapeutic goal is rapid and deep suppression of amyloidogenic light chains, ideally achieving complete response or very good partial response. Cardiac response is traditionally assessed using NT-proBNP and NYHA class: in patients with baseline NT-proBNP above 650 ng/L, a reduction greater than 30% and greater than 300 ng/L supports cardiac organ response [77,79]. However, NT-proBNP may be influenced by renal function, rhythm, congestion, and treatment effects; therefore, the thesis explores whether echocardiography and CMR can provide complementary evidence of myocardial recovery.

ATTR-specific therapy follows two major strategies: stabilization of the transthyretin tetramer and suppression of hepatic TTR production [80]. Tafamidis stabilizes the tetramer and was shown in ATTR-ACT to reduce all-cause mortality and cardiovascular hospitalizations in ATTR cardiomyopathy [81,121,123]. Diflunisal also stabilizes TTR but is limited by nonsteroidal anti-inflammatory toxicity [82,83]. Acoramidis was designed to achieve near-complete tetramer stabilization and has shown benefit in ATTR cardiomyopathy across mortality, hospitalization, functional, and biomarker endpoints [84–86].

TTR production silencers include patisiran, vutrisiran, inotersen, and emerging antisense agents such as eplontersen. Patisiran improved neuropathy in ATTRv and showed favorable cardiac effects in predefined and subsequent cardiac analyses [45,87–89]. Vutrisiran, a subcutaneous siRNA administered every three months, reduced mortality and recurrent cardiovascular events in ATTR cardiomyopathy and improved functional capacity, quality of life, and cardiac biomarkers [90,91]. Inotersen slowed neurologic progression in ATTRv but requires monitoring for thrombocytopenia and glomerulonephritis [46]. Gene-editing therapy using CRISPR-Cas9 has introduced the possibility of durable TTR knockdown after a single intervention [92,93]. Anti-fibril and amyloid-depleting therapies, including antibodies targeting non-native TTR or amyloid constituents, represent an emerging strategy aimed at clearing established deposits [94–96].

Supportive cardiovascular management remains essential across amyloid subtypes. Diuretics are the cornerstone of congestion control, but excessive preload reduction may worsen low-output physiology in restrictive cardiomyopathy [97]. Conventional guideline-directed heart failure therapies are often poorly tolerated because patients may depend on heart rate and

adequate filling pressures; beta-blockers, angiotensin-converting enzyme inhibitors, angiotensin receptor blockers, and neprilysin inhibitors may cause hypotension or clinical deterioration, particularly in autonomic dysfunction [3,31,98–100]. SGLT2 inhibitors are emerging as potentially useful adjunctive therapy, with observational data suggesting tolerability and favorable effects on congestion, diuretic requirements, hospitalization, and survival in ATTR cardiomyopathy and possible benefit in AL amyloidosis [101–103].

Arrhythmia management is particularly important. Atrial fibrillation is common, especially in ATTRwt, and amyloid atrial myopathy increases thromboembolic risk. Anticoagulation is recommended in cardiac amyloidosis with atrial fibrillation regardless of CHA2DS2-VASc score, and atrial mechanical dysfunction may also increase thrombotic risk in sinus rhythm [35,36,104]. Amiodarone is commonly used for rhythm control, while non-dihydropyridine calcium channel blockers should be avoided because of potential toxicity and worsening heart failure [105–108]. Device therapy remains individualized; pacemakers may be required for conduction disease, while defibrillator decisions are complex and depend on arrhythmic risk, amyloid subtype, stage, and competing mortality [109,110]. Advanced heart failure therapies, transplantation, and mechanical circulatory support require careful assessment of extracardiac involvement, frailty, age, and expected systemic disease trajectory [31,76,111–113].

SECTION II: PERSONAL CONTRIBUTIONS TO THE FIELD

1. Dynamic Assessment of Cardiac Involvement in ATTR Amyloidosis: From Prognosis to Disease Progression

The ATTR chapter examines cardiac involvement through three complementary perspectives: genotype-related phenotype heterogeneity, contemporary prognostic stratification, and longitudinal treatment monitoring. Across the three studies, the results show that ATTR amyloidosis cannot be adequately characterized by a single static model. Instead, prognosis and disease evolution depend on genotype, age at onset, clinical phenotype, biomarker profile, imaging severity, and access to disease-modifying therapy. The chapter first defines the Romanian Glu54Gln phenotype in comparison with major Western European ATTRv variants, then proposes a new staging system for treated hereditary ATTR, and finally demonstrates disease stability on serial echocardiography and CMR in treated ATTR cardiomyopathy.

Study 1: ATTR Variants In Eastern And Western Europe: A Phenotypic Comparison Of Romanian And French ATTRv Cohorts

The first study compared Romanian and French ATTRv cohorts to describe variant prevalence, age at onset, phenotype, cardiac involvement, and prognosis. The initial French population included 571 consecutive patients with hereditary ATTRv diagnosed between 2010 and 2023, while the Romanian population included 38 consecutive patients diagnosed between 2018 and 2023. After excluding asymptomatic carriers and patients with unknown or homozygous allele status, 321 French and 33 Romanian patients remained eligible. The Romanian cohort was dominated by Glu54Gln, which accounted for 78.8% of Romanian cases. In the French cohort, the most frequent variants were Val122Ile, Val30Met, and Ser77Tyr. For comparative analysis, the study focused on variant groups with sufficient sample size: Glu54Gln (n=26), Val122Ile (n=200), late-onset Val30Met (n=30), early-onset Val30Met (n=17), and Ser77Tyr (n=18).

Results

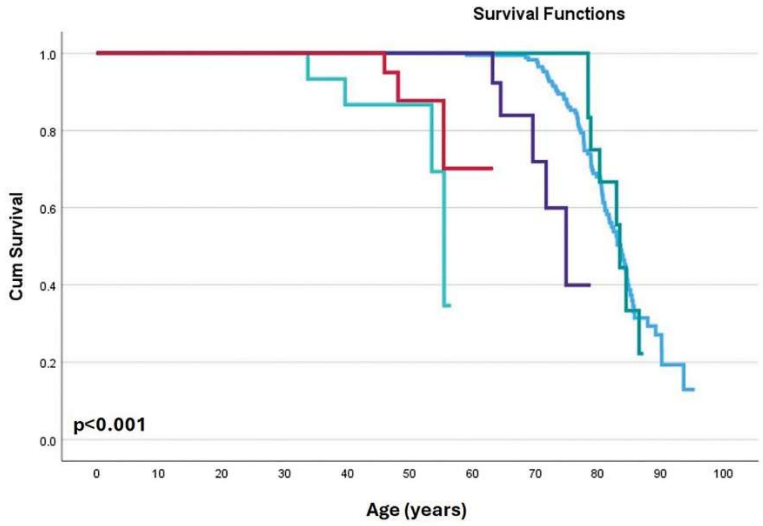
The results demonstrated marked genotype-related heterogeneity in age at diagnosis and symptom onset. Glu54Gln patients were diagnosed at a median age of 46 years [42–50],

substantially younger than Val122Ile patients, diagnosed at 76 years [71–80], and late-onset Val30Met patients, diagnosed at 70 years [61–76]. Early-onset Val30Met remained the youngest group, with diagnosis at 37 years [27–46], while Ser77Tyr patients were diagnosed at 58 years [55–68]. Extracardiac symptoms also appeared early in Glu54Gln, with a median onset age of 44 years [40–47], compared with 68 years [61–74] in Val122Ile and 64 years [57–73] in late-onset Val30Met. The delay between extracardiac symptom onset and diagnosis was shorter in Glu54Gln than in Val122Ile, but still clinically important, with a median of 22 months [10–48]. The pattern of initial extracardiac manifestations distinguished Glu54Gln from the main Western European cardiac variants. In the Glu54Gln group, symptomatic dysautonomia was the first extracardiac manifestation in 50% of patients, while peripheral neuropathy was first in 38.5%. This contrasted sharply with Val122Ile, where carpal tunnel syndrome was the dominant first extracardiac manifestation, occurring in 66.3% of patients, and peripheral neuropathy was less frequent as an initial sign. Early-onset Val30Met was more neurologic, with peripheral neuropathy as the first extracardiac symptom in 81.3% of cases. These results show that Glu54Gln has a mixed phenotype, with early autonomic and peripheral nerve involvement rather than an exclusively cardiac presentation.

Cardiac manifestations also occurred early in Glu54Gln. Median age at cardiac symptom onset was 45 years [42–49], compared with 74 years [69–79] for Val122Ile, 69 years [60–76] for late-onset Val30Met, 39 years [37–46] for early-onset Val30Met, and 56 years [54–61] for Ser77Tyr. Heart failure symptoms were the first cardiac manifestation in 61.5% of Glu54Gln patients, similar to Val122Ile (59.7%) and higher than early-onset Val30Met (15.4%). Conduction disorder as the first cardiac manifestation was most frequent in early-onset Val30Met (76.9%), whereas Glu54Gln showed a lower prevalence (11.5%). Documented atrial fibrillation was relatively uncommon in Glu54Gln (7.7%) compared with Val122Ile (22.5%), and pacemaker implantation was also infrequent (3.8%).

Biomarker and imaging results further clarified the Glu54Gln phenotype. NT-proBNP values were elevated in Glu54Gln, with a median of 1720 ng/L [543–3845], but the proportion of patients with elevated troponin was lower than in Val122Ile. Echocardiography showed that interventricular septal thickness in Glu54Gln was 16 mm [14–18], comparable to Val122Ile and other cardiac or mixed variants, while left ventricular ejection fraction was 54% [45–58] and GLS was impaired at 12% [10–15] in absolute value. Left atrial volume was increased, and E/e′ suggested elevated filling pressures. Bone scintigraphy showed myocardial uptake in 100% of Glu54Gln patients, supporting a high prevalence of cardiac involvement despite the mixed neurologic-autonomic presentation.

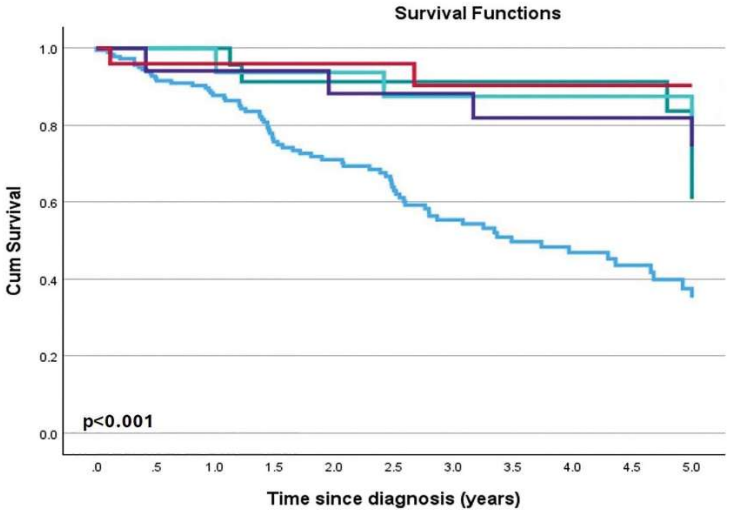
A



	Estimated survival Mean (years)	95% CI	Median Survival (years)	95% CI	Pairwise comparison of Glu54Gln (p value)
Glu54Gln	59.856	[56.490 – 63.252]	-	-	
Val122Ile	83.638	[82.210 - 85.067]	83.570	[81.588 - 85.552]	< 0.001
late-onset Val30Met	83.161	[81.211 - 85.112]	83.427	[81.962 - 84.893]	0.005
early-onset Val30Met	52.949	[49.537 - 56.362]	55.403	[52.521 - 58.285]	0.249
Ser77Tyr	73.632	[70.294 - 76.970]	74.863	[68.753 - 80.973]	0.041

Figure 3A. Survival analysis. A. Kaplan Meier curves showing survival in years. Time to 50% survival was almost identical for Val122Ile (83,5 years) and Val30Met late onset form (83,4 years); while early-onset Val30Met had a median survival of 55,4 years and Ser77Tyr 74,8 years. Due to low number of events for the Glu54Gln group time to 75% survival was calculated at 55.3 years.

B



Number at risk

	Year 0	Year 1	Year 2	Year 3	Years 4	Year 5
Glu54Gln	23	19	17	13	7	1
Val122Ile	172	120	77	45	26	8
late-onset Val30Met	25	22	17	15	13	7
early-onset Val30Met	17	16	15	13	12	7
Ser77Tyr	18	16	14	13	11	6

Figure 3B. Survival analysis. B. Kaplan-Meier curves illustrating survival at 5 years after diagnosis; pairwise comparison showed significantly lower survival rates for Val122Ile.

Survival analysis produced two complementary interpretations. When survival was analyzed according to absolute age, Glu54Gln had a lower estimated survival age than Val122Ile and late-onset Val30Met because disease began much earlier. However, when survival was calculated from diagnosis, Glu54Gln patients had a favorable five-year survival probability of 0.90 ± 0.06. This was significantly higher than Val122Ile, which had a five-year survival probability of 0.35 ± 0.05, and similar to early-onset Val30Met, late-onset Val30Met, and Ser77Tyr. Therefore, the study suggests that Glu54Gln is aggressive because of early onset and multisystem involvement, but survival after diagnosis may be relatively preserved compared with older cardiac Val122Ile patients.

The main result of this study is the demonstration that Eastern and Western European ATTRv populations differ substantially. The Romanian Glu54Gln variant is characterized by early onset, autonomic and neurologic involvement, frequent cardiac disease, high scintigraphic uptake, and a mixed clinical trajectory. These findings have practical consequences for genetic counseling and surveillance: Glu54Gln carriers should be followed earlier than carriers of late-onset cardiac variants, and surveillance should include both neurologic and cardiac assessment.

Discussion points

This study should be interpreted in the context of the changing epidemiology of ATTRv in Europe. Data from THAOS have clarified the distribution of TTR variants in Western Europe, but Eastern European populations have historically been underrepresented [114,115]. The Romanian data therefore add important regional information by showing that Glu54Gln is not merely a rare local variant but a founder-like mutation with a recognizable clinical profile. The overall prevalence of ATTRv in Romania remains lower than in classic endemic regions such as northern Portugal, but the north-eastern Romanian cluster has a higher local prevalence than the national estimate [27,116].

The comparison with the French cohort also illustrates how referral patterns and population movements influence apparent genotype distribution. Earlier French ATTRv descriptions emphasized Val30Met and Ser77Tyr, whereas more recent cohorts show increasing Val122Ile diagnoses, likely related to improved cardiology-driven detection and demographic factors [114,118]. In contrast, the Romanian ATTRv population is dominated by Glu54Gln, with smaller contributions from other variants such as Glu89Lys, Glu89Val, and Ile107Val [27,117]. These differences support the need for country- or region-specific diagnostic awareness rather than extrapolation from Western European registries.

The Glu54Gln phenotype appears mixed and aggressive because neurologic, autonomic, and cardiac manifestations develop early and often overlap. Its closest phenotypic comparator was Ser77Tyr, but Glu54Gln onset occurred more than a decade earlier. This is clinically important for genetic counseling: carriers of Glu54Gln should probably enter structured follow-up earlier than carriers of late-onset cardiac variants, potentially beginning around the age of 36, in line with principles of targeted follow-up for TTR mutation carriers [119]. Surveillance should include neurologic, autonomic, cardiac biomarker, ECG, echocardiographic, and scintigraphic assessment, rather than focusing exclusively on cardiomyopathy.

The survival findings must be interpreted cautiously. Val122Ile patients had poorer survival after diagnosis, but they were also older and likely carried more comorbidity, including diabetes, atherosclerosis, and other cardiovascular disease [120]. Conversely, Glu54Gln patients had lower survival age because disease onset was much earlier, not necessarily because survival after diagnosis was worse. The number of events in the Glu54Gln, Ser77Tyr, and Val30Met groups was limited, preventing precise variant-specific mortality estimates. Differences in diagnostic timing, access to tafamidis or gene silencers, and local device practices may also have influenced prognosis [81].

Study 2. A New Staging System for Hereditary ATTR in the Era of Specific Therapies

The second ATTR study addressed whether existing prognostic systems remain adequate for hereditary ATTR in the era of disease-modifying therapy. The total population included 396 treated ATTRv patients, randomly divided into a score derivation cohort of 258 patients and an internal validation cohort of 138 patients. The derivation cohort had a median age of 69.9 years [59.4–77.1], 65.9% men, and 55.0% cardiac variants. Phenotypes were heterogeneous: 147 patients had cardiac variants, 94 had mixed cardiac-neurologic phenotypes, and 17 had predominantly neurologic phenotypes. The most frequent variants were Val122Ile (52.33%), Val30Met (16.67%), and Glu54Gln (7.75%).

Results

The baseline profile confirmed that cardiac phenotype patients had more advanced cardiac disease than mixed or neurologic phenotype patients. In the derivation cohort, patients with cardiac variants were older, more often male, and had more heart failure symptoms at diagnosis. They had higher NT-proBNP values, higher hs-TnT values, lower eGFR, thicker ventricular walls, lower ejection fraction, worse GLS, lower stroke volume index, higher filling pressures, and more right ventricular impairment. Heart failure hospitalization during five-year

follow-up was much more frequent in the cardiac phenotype group than in mixed or neurologic phenotypes, supporting the prognostic importance of cardiac involvement.

The National Amyloidosis Centre staging system was applied first. In the derivation cohort, 159 patients (61.6%) were NAC stage I, 62 (24.0%) were stage II, and 37 (14.3%) were stage III. NAC stage I patients had a five-year survival rate of 74.4%, whereas stage II and stage III patients had similar five-year survival rates, 52.2% and 55.2%, respectively. The log-rank comparison showed that stage I differed from stage II, but stage II and stage III did not separate meaningfully. Cox regression confirmed increased mortality risk for stage II and stage III compared with stage I, but Harrell's C-statistic was only 0.598. These results showed that NAC staging partly identified lower-risk patients but did not adequately discriminate intermediate from advanced risk in treated hereditary ATTR.

Table 1. Univariate and multivariate predictors of mortality in the Score Derivation Cohort

Univariate	**HR**	**95% CI**	**p**
Age (years)	1.088	1.056 - 1.120	<0.001
< 65	1 (Ref)	-	-
≥ 65	11.436	4.132 - 31.610	<0.001
NYHA III-IV functional class at diagnosis	2.452	1.445 - 4.161	<0.001
NT-proBNP	1.002	1.001 - 1.003	<0.001
hs-TnT, ng/L	1.008	1.005 - 1.011	<0.001
eGFR (CKD-EPI), mL/min/1.73 m^2	1.025	1.013 - 1.034	<0.002
GGT, UI/L	1.003	1.001 - 1.005	<0.001
Interventricular septum thickness, mm	1.126	1.054 - 1.202	<0.001
LV global longitudinal strain, %	1.276	1.156 - 1.271	<0.001
TAPSE, mm	1.152	1.085 - 1.176	<0.001
Pericardial effusion	1.843	1.111 - 3.060	0.018
Multivariate			
NT-proBNP ng/L	1.002	1.001 - 1.003	0.028
eGFR (CKD-EPI), mL/min/1.73 m^2	1.012	1.001 - 1.024	0.044
GLS %	1.210	1.094 - 1.248	<0.001

Considered correlations between predictors: NYHA III-IV functional class at diagnosis and NT-proBNP ($p < 0.001$, Cramér's V $\chi 2 = 6.641$); eGFR (CKD-EPI) and Age ($p < 0.001$, Pearson's $R=0.605$)

Univariate and multivariate analyses identified NT-proBNP, eGFR, and GLS as key predictors of mortality. A combined model including GLS, NT-proBNP, and eGFR performed better than single-variable or two-variable models. Optimal cut-off values were identified and then rounded for clinical usability: NT-proBNP ≥2000 ng/L, eGFR ≤65 mL/min/1.73 m^2, and GLS ≥−11%. These thresholds were significantly associated with mortality. Stage I was defined by the absence of all three criteria. Stage III required the GLS criterion plus either NT-proBNP or eGFR abnormality, while all remaining combinations were classified as Stage II.

The new staging system produced strong survival separation in the derivation cohort. Sixty-eight patients (26.4%) were classified as Stage I, 103 (39.9%) as Stage II, and 87 (33.7%) as Stage III. Five-year survival was 98.5% in Stage I, 75.1% in Stage II, and 29.4% in Stage III. Median survival for Stage III was 3.61 years. Compared with Stage I, the hazard ratio for death was 13.47 for Stage II and 54.3 for Stage III. After adjustment for age, the model remained strongly prognostic, with an age-adjusted hazard ratio of 9.9 for Stage II and 39.75 for Stage III compared with Stage I. The hazard ratio for Stage III compared with Stage II was 4.03. The model had a Harrell C-statistic of 0.733 and outperformed NAC staging.

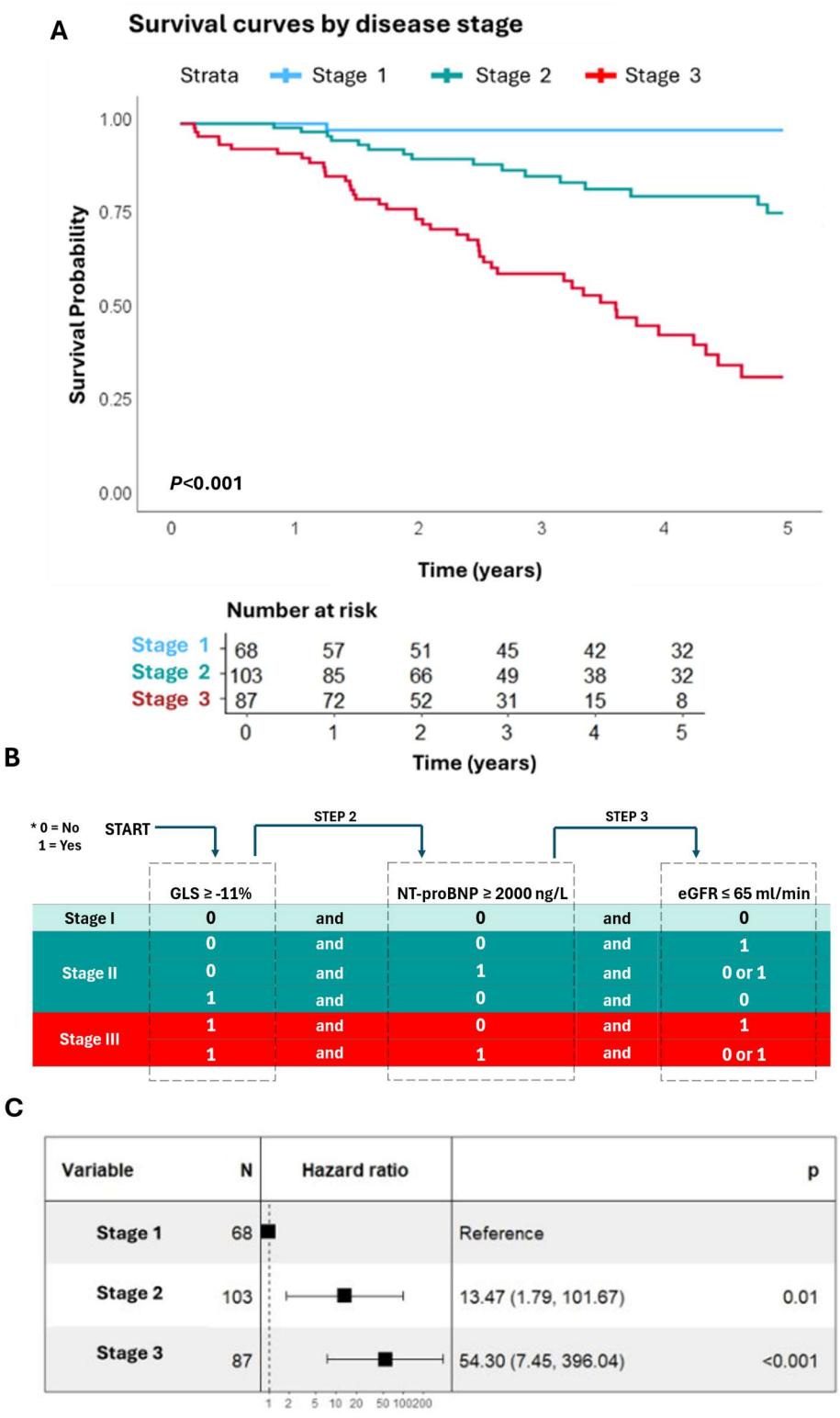


Figure 4. A. Kaplan–Meier curves showing survival probabilities in 258 patients with ATTRv stratified by disease stage (log-rank test; Stage 1 vs. Stage 2, $P = 0.001$; Stage 2 vs. Stage 3, $P < 0.001$). Median survival for Stage 3 patients was 3.6 years (95% CI 3.0 - 4.2 years). **B.** Definition of disease stages based on the 3 criteria: GLS ≥ -11%, NT-proBNP ≥ 2000 ng/L and eGFR ≤ 65 ml/min/1,73m^2. **C.** By Cox proportional hazards regression analysis, compared with Stage 1, the HR for death was 13.47 (95% CI 1.79–101.67, $P = 0.001$) for Stage 2 and 54.3 (95% CI 7.45–396.04, $P < 0.001$) for Stage 3 patients. Harrell's *c*-statistics was 0.752. Schoenfeld Residuals were used to assess goodness of fit, P=0.406.

Formal comparison with NAC staging confirmed better discrimination. The AUC for the NAC model was 0.653, whereas the AUC for the new staging system was 0.804, with a statistically significant difference by DeLong's test. This result is central to the thesis because it shows that adding an imaging parameter—GLS—to established biomarker and renal markers improves risk stratification in treated hereditary ATTR.

Internal validation confirmed the model. In the validation cohort, 42 patients (30.4%) were Stage I, 38 (27.5%) Stage II, and 45 (32.6%) Stage III. Five-year survival was 94.1% in Stage I, 76.2% in Stage II, and 38.4% in Stage III, with significant separation between Stage I and Stage II and between Stage II and Stage III. Median survival for Stage III was 2.6 years. Cox regression showed increased mortality risk for Stage II and Stage III compared with Stage I, and Harrell's C-statistic was 0.747. Subgroup analyses showed that the system was useful in both cardiac and mixed cardiac-neurologic phenotypes, although event numbers limited some subgroup estimates.

The study also explored the effect of treatment access. Patients diagnosed before 2018 had a longer delay to treatment initiation than those diagnosed after 2018. Although the global comparison before versus after 2018 did not show a statistically significant survival difference, additional analysis suggested better prognosis when diagnosis-to-treatment delay was two years or less. Stage III patients with early access to treatment had a longer median survival than Stage III patients with delayed treatment. This finding reinforces the importance of early diagnosis and rapid initiation of disease-specific therapy.

The main result of this study is the development and internal validation of a clinically practical staging system for treated hereditary ATTR. By combining NT-proBNP, eGFR, and GLS, the model captures myocardial stress, renal-systemic involvement, and myocardial deformation. It is therefore better adapted to contemporary ATTRv care than biomarker-only models developed before widespread use of specific therapy.

Discussion points

The main discussion point of this study is that available ATTR staging systems were developed before widespread use of specific therapy and may not fully apply to treated hereditary ATTR. The Mayo ATTR system was derived in wild-type ATTR and uses NT-proBNP and troponin T [11]. The NAC system was derived in a mixed ATTR population, with a predominance of ATTRwt and relatively limited representation of non-Val122Ile hereditary variants [9]. In the present treated ATTRv cohort, the NAC system separated lower-risk patients

but failed to distinguish stage II from stage III, suggesting that contemporary treated hereditary disease requires a more nuanced model.

The proposed model integrates two established systemic and cardiac biomarkers, NT-proBNP and eGFR, with one imaging marker, GLS. NT-proBNP reflects myocardial stress, while eGFR captures renal function and systemic vulnerability, both already recognized in ATTR prognosis [9,11]. GLS adds direct information on myocardial deformation and has gained increasing prognostic relevance in cardiac amyloidosis and in post hoc analyses of ATTR clinical trial populations [125,127]. The improved discriminatory performance of the new model supports the thesis argument that imaging should not remain secondary to biomarker staging but should be incorporated into contemporary risk assessment.

Treatment status is central to interpretation. Tafamidis has been associated with improved outcomes in ATTR cardiomyopathy, and THAOS data show better survival among tafamidis-treated patients compared with untreated patients [122,123]. In the present cohort, almost all patients received disease-specific treatment, but dose, access, treatment delay, and switching to gene silencers varied. This reflects real-world practice and increases clinical relevance, but also introduces heterogeneity. The observation that early access to therapy was associated with better prognosis reinforces the importance of timely diagnosis and treatment initiation.

The staging system also highlights the complexity of genotype and phenotype. Cardiac-dominant variants were older and had more advanced cardiac involvement, whereas mixed or neurologic phenotypes had different risk profiles. Because ATTRv onset age and organ expression vary substantially by mutation [114,115], a staging system for hereditary ATTR must work across phenotypes without depending exclusively on genotype. The proposed model achieved this by focusing on measurable cardiac and systemic consequences rather than variant identity alone.

Important limitations remain. The study was retrospective, treatment regimens were heterogeneous, and external validation was not available. The neurologic component of ATTRv was not fully integrated because standardized measures of autonomic or neurologic severity were not consistently available, even though autonomic dysfunction may influence prognosis through hypotension, cachexia, and systemic frailty [128]. Future validation should test the model in independent cohorts, assess longitudinal stage migration, and determine whether changes in GLS, NT-proBNP, or eGFR under therapy predict progression or treatment failure.

Study 3: Serial Multimodality Imaging Demonstrates Disease Stability In Transthyretin Cardiac Amyloidosis Receiving Contemporary Disease-Modifying Therapies

The third ATTR study prospectively evaluated serial biomarkers, echocardiography, and CMR in 19 patients with ATTR cardiomyopathy receiving contemporary disease-modifying therapy. The cohort included 11 men (57.9%) and 8 women (42.1%), with a median age of 51.0 years [42.5–78.8]. Fourteen patients (73.7%) had hereditary ATTR and five (26.3%) had wild-type ATTR. Among ATTRv patients, Glu54Gln predominated (n=12), while two patients carried Glu89Val. At inclusion, 10 patients (52.6%) were receiving patisiran and 9 (47.4%) tafamidis. According to NAC staging, 11 patients (57.9%) were stage I and 8 (42.1%) stage II. Baseline NT-proBNP was 2216.5 ng/L [367.3–4080.8], and hs-cTnI was 8.17 ng/L [4.57–31.0]. The cohort reflects contemporary practice, with high use of supportive heart failure therapy. SGLT2 inhibitors were prescribed in 73.7%, loop diuretics in 84.2%, and mineralocorticoid receptor antagonists in 31.6%. This is relevant for interpreting follow-up because changes in stroke volume, NT-proBNP, or congestion-related measures may reflect both amyloid-specific therapy and optimization of volume status.

Results

Repeat echocardiography was performed after a median follow-up of 16.9 months [12.3–23.7]. The main result was stability of cardiac structure and function. Interventricular septal thickness remained unchanged at 15.0 mm at baseline and follow-up (p=0.835). LV end-diastolic volume remained stable, and LVEF showed no significant decline, remaining approximately 54–55%. GLS showed a favorable numerical trend, from −13.6% to −14.2%, but this was not statistically significant (p=0.647). Stroke volume index increased significantly from 32.3 to 35.6 mL/m² (p=0.020), suggesting improved forward flow or hemodynamic optimization during follow-up.

Diastolic and atrial parameters were also stable. Average e′ velocity, E/e′ ratio, left atrial volume index, and left atrial reservoir strain did not change significantly. Right ventricular parameters were preserved: TAPSE remained stable, RV S′ showed no significant change, and RV free-wall and global strain demonstrated favorable numerical trends without statistical significance. Thus, serial echocardiography did not show the expected pattern of progressive wall thickening, worsening systolic function, declining strain, or increasing filling pressure that would be anticipated in untreated progressive ATTR cardiomyopathy.

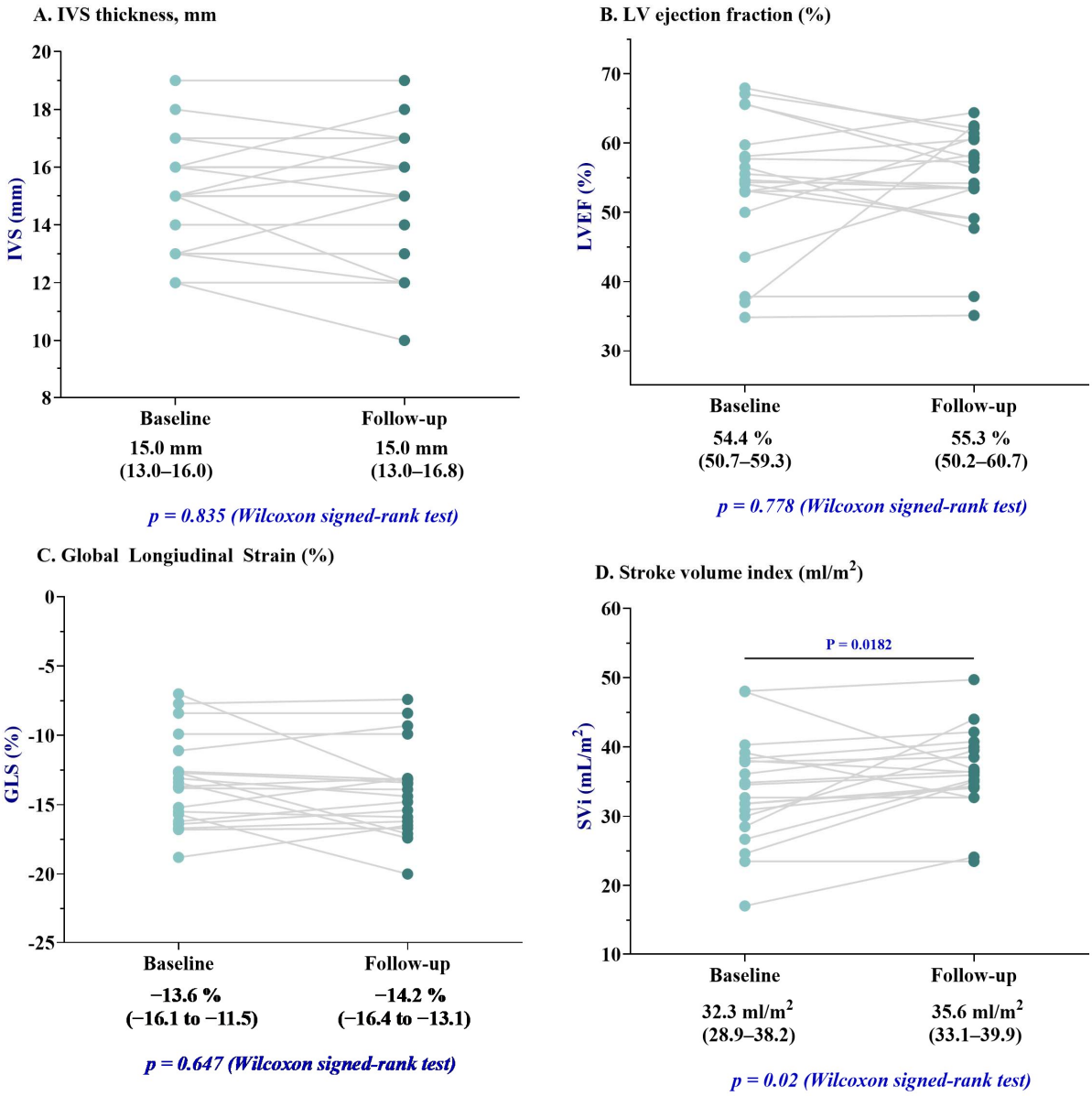


Figure 5. Paired echocardiographic assessment at baseline and follow-up in patients with transthyretin cardiac amyloidosis receiving disease-modifying therapy. Panels show changes in (A) IVS thickness, (B) LVEF, (C) GLS, and (D) SVi. Values beneath each panel are presented as median (IQR). Boxes represent paired differences with corresponding 95% confidence intervals. P values were derived from paired-sample analyses.

Serial CMR confirmed the echocardiographic impression of disease stability. LV end-diastolic volume index remained stable, from 86.0 to 85.6 mL/m² (p=0.279), and LV end-systolic volume index also showed no significant change. LVEF remained stable, and maximal wall thickness was unchanged, from 16.5 to 16.0 mm (p=0.500). Tissue characterization parameters showed no significant progression: native T1 changed from 1138.0 to 1152.1 ms

(p=0.094), ECV from 53.5% to 55.8% (p=0.171), and T2 remained stable at approximately 50 ms (p=0.758). Right ventricular volumes and ejection fraction were also unchanged.

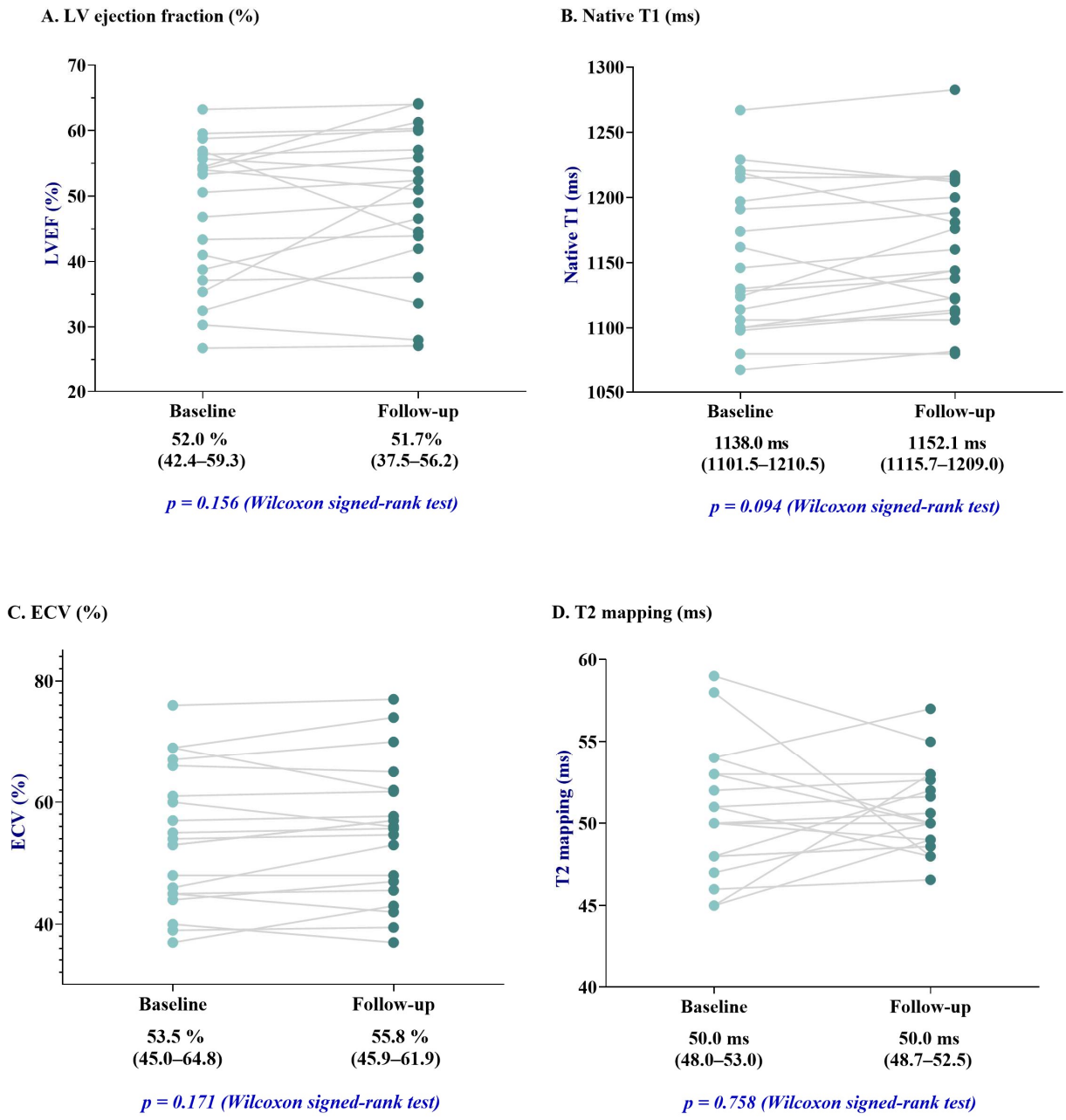


Figure 6. Serial CMR assessment demonstrates preservation of ventricular function and myocardial tissue characteristics. Individual paired measurements obtained at baseline and follow-up are shown for left ventricular ejection fraction (A), native T1 mapping (B), extracellular volume fraction (C), and T2 mapping (D). Data are expressed as median (interquartile range), and comparisons were performed using the Wilcoxon signed-rank test. No significant changes were observed over time, consistent with imaging evidence of disease stability.

The most important result is not regression but absence of progression. In ATTR cardiomyopathy, untreated disease is expected to progress through increasing amyloid burden, rising ECV, worsening deformation, increasing wall thickness, and declining functional capacity. In this cohort, ventricular structure, biventricular function, wall thickness, and CMR tissue markers remained stable over approximately 17 months. The study therefore supports disease stabilization as a clinically meaningful treatment target in ATTR cardiomyopathy and positions serial multimodality imaging as a tool to document therapeutic effect beyond biomarkers alone.

Discussion points

The central discussion point of the serial ATTR imaging study is that disease stability may represent therapeutic success. Untreated ATTR cardiomyopathy usually progresses through increasing amyloid burden, rising NT-proBNP, increasing wall thickness, worsening myocardial deformation, declining functional capacity, and progressive CMR abnormalities. Longitudinal CMR data have shown that untreated patients may demonstrate increases in ECV, ventricular wall thickness, and biomarkers, while treatment with patisiran has been associated with stability or regression in selected cohorts [87,129]. Therefore, the absence of significant deterioration in this study is clinically meaningful, even if overt regression was not observed.

CMR tissue characterization is particularly important because native T1 and ECV are less dependent on loading conditions than many echocardiographic or biomarker parameters. ECV is considered a marker of amyloid burden and has prognostic significance in ATTR amyloidosis [130]. In this cohort, stability of native T1, ECV, and T2 suggests that disease-modifying therapy may have attenuated the expected progression of myocardial infiltration. This interpretation is stronger than relying on NT-proBNP alone, because natriuretic peptide changes may be influenced by congestion, renal function, rhythm, and diuretic or SGLT2 inhibitor therapy.

The widespread use of SGLT2 inhibitors deserves specific interpretation. Observational data suggest that SGLT2 inhibitors are generally well tolerated in ATTR cardiomyopathy and may be associated with lower heart failure hospitalization, cardiovascular mortality, and all-cause mortality [102]. Smaller real-world studies also suggest tolerability in AL and ATTR amyloidosis, with favorable effects on congestion and cardiorenal parameters [103]. In the present study, improved stroke volume index and stable biomarkers may therefore reflect both ATTR-specific therapy and improved volume management. This does not weaken the findings

but supports the need to interpret serial imaging and biomarkers within the full therapeutic context.

The inclusion of both tafamidis- and patisiran-treated patients reflects contemporary practice but limits comparison between mechanisms. Tafamidis stabilizes transthyretin and has demonstrated survival benefit in ATTR cardiomyopathy [81,123], while patisiran and other gene silencers reduce hepatic TTR production and have shown cardiac structural or biomarker effects in selected studies [45,87–89]. The cohort was not powered to compare stabilizers and silencers, but the similar pattern of imaging stability supports the broader concept that both strategies may attenuate progression. Longer follow-up and larger cohorts are needed to evaluate whether stabilization persists and whether specific imaging markers can identify early progression despite therapy.

2. Dynamic Assessment of Cardiac Involvement in Light-Chain Amyloidosis: From Prognosis to Organ Response

The AL chapter focuses on results from two studies addressing different phases of cardiac AL amyloidosis. The first study evaluates prognosis at diagnosis and shows that right ventricular dysfunction identifies an ultra-high-risk subgroup beyond established biomarker staging. The second study evaluates longitudinal response after daratumumab-based therapy and shows that biomarker improvement may be accompanied by echocardiographic and CMR evidence of myocardial reverse remodeling. Together, the studies support a dynamic model in which imaging improves both baseline risk stratification and follow-up assessment of cardiac organ response.

Study 1. Incorporating Right Ventricular Function into the European Modified Mayo Staging System

The first AL study included 92 patients with newly diagnosed systemic light-chain amyloidosis and cardiac involvement evaluated between 2018 and 2023. The cohort had advanced cardiac disease at presentation. Median age was approximately 61 years [54.5–67.5], and 62% were male. Median NT-proBNP was 6340.5 ng/L [2323.8–13176.2], troponin I was 0.1 ng/mL [0.0–0.3], and eGFR was 66.9 mL/min/1.73 m² [38.4–91.6]. Echocardiography

showed increased interventricular septal thickness, median 15.5 mm [14.0–18.0], impaired LVEF at 51.0% [38.8–57.9], and impaired GLS at −11.4% [−14.2 to −7.9].

Table 2. Baseline Characteristics of the AL Amyloidosis Cohort

Variable	Value
Age at diagnosis, years	61.0 (54.5–67.5)
Male sex, n (%)	57 (62.0%)
NT-proBNP, ng/L	6340.5 (2323.8–13176.2)
Troponin I, ng/mL	0.1 (0.0–0.3)
eGFR, mL/min/1.73m²	66.9 (38.4–91.6)
IVS thickness, mm	15.5 (14.0–18.0)
LVEF, %	51.0 (38.8–57.9)
GLS, %	−11.4 (−14.2 to −7.9)
RV basal diameter, mm	35.2 (31.0–39.0)
TAPSE, mm	16.0 (12.0–19.0)
RV S', cm/s	10.0 (8.0–12.0)
FAC, %	35.0 (29.5–41.5)
RV global strain, %	−13.5 (−16.9 to −10.3)
RV free wall strain, %	−16.9 (−22.3 to −13.1)
Follow-up, months	30.3 (3.4–61.0)
All-cause mortality, n (%)	47 (51.1%)

Values are presented as median (interquartile range) or number (percentage), as appropriate.

The European modified Mayo staging distribution confirmed high-risk disease: 25 patients (27%) were stage II, 26 patients (28%) were stage IIIA, and 41 patients (45%) were stage IIIB. No patients were stage I, reflecting the advanced referral profile of the cohort. Right ventricular dysfunction was common. Median TAPSE was 16.0 mm [12.0–19.0], RV S′ was 10.0 cm/s [8.0–12.0], RV global strain was −13.5% [−16.9 to −10.3], and RV free-wall strain was −16.9% [−22.3 to −13.1]. During follow-up, 47 patients (51.1%) died, confirming the severe prognosis of this population.

Both TAPSE and RV S′ were associated with mortality, but TAPSE provided stronger prognostic performance and was selected for integration into the staging model. TAPSE and RV S′ were strongly correlated (R=0.751), suggesting that both reflected right ventricular longitudinal function. However, TAPSE remained independently associated with overall

survival in multivariable analysis after adjustment for Mayo stage and LVEF. In this model, Mayo stage remained prognostic, with higher risk in stage IIIA and IIIB compared with stage II, whereas LVEF was not independently associated with survival. This finding supports the view that right ventricular longitudinal dysfunction captures advanced hemodynamic and myocardial disease not fully reflected by left ventricular ejection fraction.

The optimal TAPSE threshold for survival discrimination was 14 mm, identified using the Contal and O'Quigley method. TAPSE below 14 mm had a sensitivity of 78.7% and specificity of 62.2% for mortality prediction. Kaplan–Meier analysis showed significantly worse survival in patients below this threshold. The threshold was then incorporated into the European modified Mayo framework to define a new stage IIIC in patients with severe biomarker elevation and right ventricular dysfunction.

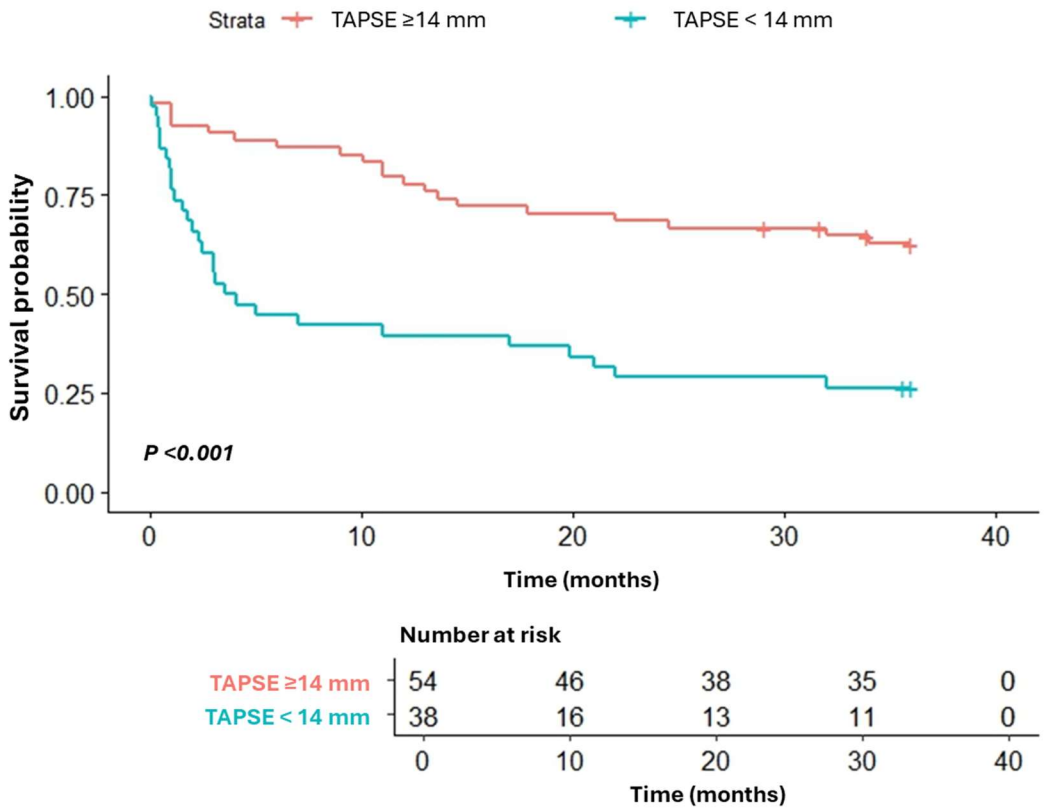


Figure 7. Kaplan–Meier curves showing survival probabilities in 92 patients with AL stratified by optimal cut-off point for TAPSE, established using the approach of Contal and O'Quigley.

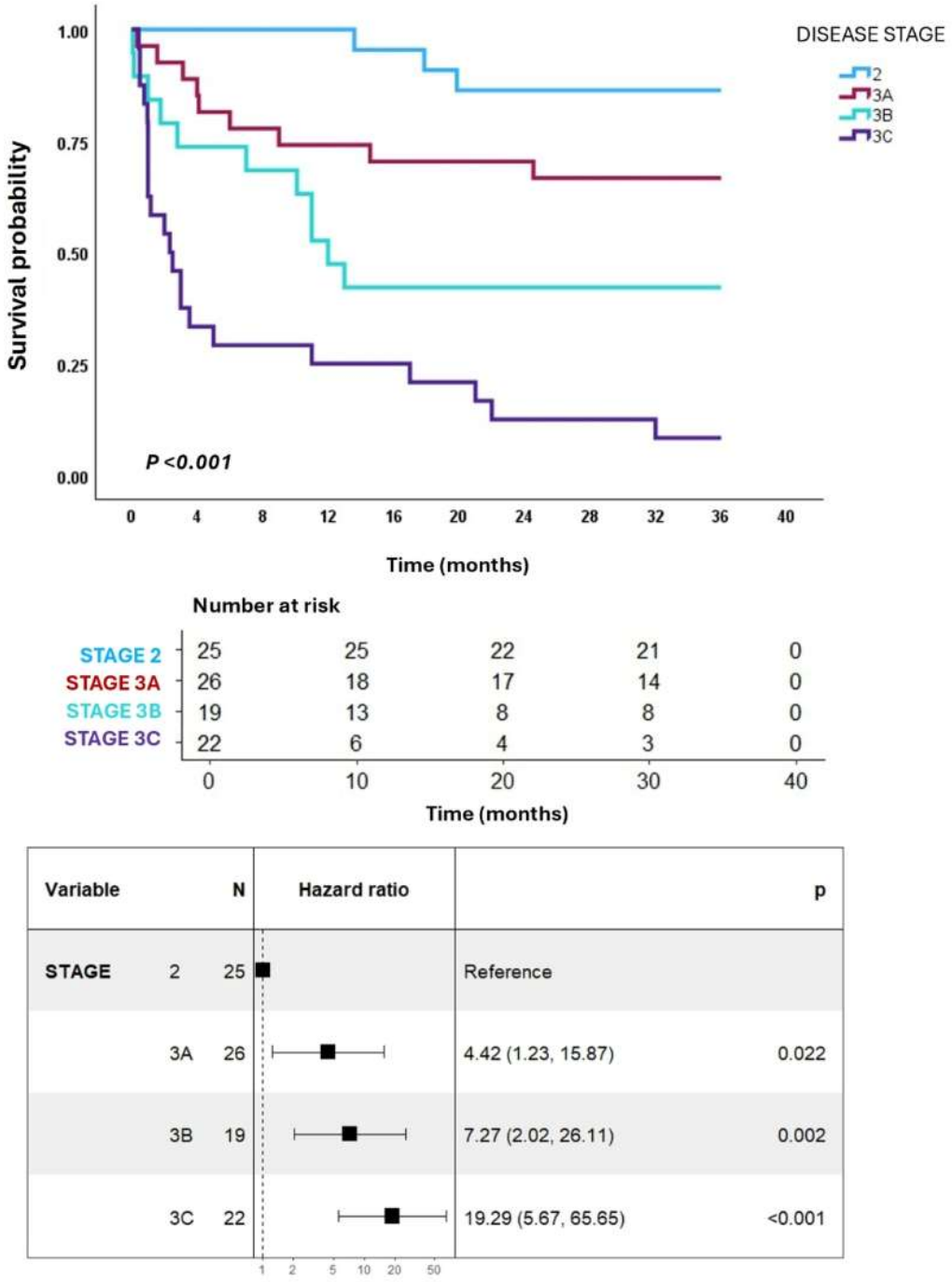


Figure 8. Kaplan–Meier survival curves according to the extended European modified Mayo staging system incorporating TAPSE <14 mm. Patients classified as Stage IIIC demonstrated significantly reduced survival compared with the remaining disease stages (log-rank p<0.001). Pairwise comparisons demonstrated significant survival differences between Stage II and Stage IIIA (p=0.022), Stage IIIA and Stage IIIB (p=0.002), and Stage IIIB and Stage IIIC (p<0.001). Mean survival was 33.4 months (95% CI 30.7–36.2 months) for Stage II patients, 26.5 months (95% CI 21.2–31.8 months) for Stage IIIA patients, 18.8 months (95% CI 12.0–25.6 months) for Stage IIIB patients, and 8.5 months (95% CI 3.8–13.2 months) for Stage IIIC patients. By Cox proportional hazards regression analysis, compared with Stage II disease, the hazard ratio (HR) for death was 4.42 (95% CI 1.23–15.87; p=0.022) for Stage IIIA patients, 7.27 (95% CI 2.02–26.11; p=0.002) for Stage IIIB patients, and 19.29 (95% CI 5.67–65.65; p<0.001) for Stage IIIC patients. Harrell's c-statistic for the final model was 0.754.

The extended staging model produced clear and progressive survival separation. Mean survival was 33.4 months in stage II, 26.5 months in stage IIIA, 18.8 months in stage IIIB, and only 8.5 months in stage IIIC. Median survival was 12.0 months for stage IIIB but only 2.3 months for stage IIIC. Twelve-month survival probability in stage IIIC was 22.7%, demonstrating dramatic early mortality once severe right ventricular dysfunction was present. Cox regression showed progressively increasing mortality risk compared with stage II: HR 4.42 for stage IIIA, HR 7.27 for stage IIIB, and HR 19.29 for stage IIIC. The final model had a Harrell C-statistic of 0.754.

The key result is the identification of an ultra-high-risk AL subgroup using a simple echocardiographic marker. TAPSE below 14 mm adds prognostic information beyond biomarkers and LVEF, improves discrimination within advanced Mayo stages, and identifies patients with a very short survival window. Clinically, this could support urgent treatment prioritization, closer early monitoring, discussion in expert centers, and more precise stratification in clinical trials. The limitation is that the proposed stage IIIC requires external validation, but the strength of the survival gradient supports the biological and clinical relevance of right ventricular dysfunction in advanced cardiac AL amyloidosis.

Discussion points

The discussion of this study centers on the prognostic importance of right ventricular dysfunction in advanced cardiac AL amyloidosis. Earlier work showed that reduced TAPSE in AL amyloidosis was associated with higher NT-proBNP, more severe left ventricular involvement, and worse survival, and that TAPSE could be one of the most clinically useful echocardiographic markers of prognosis [135]. Subsequent studies demonstrated that right ventricular longitudinal impairment reflects advanced myocardial disease and may be independently associated with mortality [136]. The present results are consistent with this literature and extend it by integrating TAPSE into an established biomarker staging system.

Right ventricular dysfunction in cardiac amyloidosis probably reflects several interacting mechanisms rather than isolated right ventricular amyloid deposition. These include biventricular infiltration, ventricular interdependence, elevated left-sided filling pressures, pulmonary hypertension, impaired longitudinal myocardial mechanics, and advanced restrictive physiology. Studies across AL and ATTR amyloidosis have shown that TAPSE and right ventricular-pulmonary artery coupling are associated with adverse outcomes [134,137]. Therefore, TAPSE may function as an integrated marker of myocardial disease burden and hemodynamic compromise.

The proposed stage IIIC has important clinical implications. In advanced AL amyloidosis, early mortality remains substantial even though modern plasma cell-directed therapies have improved hematologic response rates [5,75,77,78]. Identifying patients with median survival measured in weeks to months may help clinicians intensify monitoring, initiate urgent therapy when feasible, consider inpatient treatment, and discuss prognosis more accurately. TAPSE is inexpensive, widely available, and reproducible, making it attractive for bedside risk refinement in centers that may not have immediate access to advanced imaging.

However, the model should be interpreted cautiously. The study was retrospective, sample size was limited, and survival analyses were censored at 36 months. The number of variables that could be included in multivariable models was restricted, so the incremental value of TAPSE beyond GLS, CMR parameters, or other right ventricular strain measures could not be fully explored. External validation is therefore essential before adopting stage IIIC as a formal clinical category. Nevertheless, the marked survival gradient suggests that right ventricular assessment should be systematically included in the evaluation of cardiac AL amyloidosis.

Study 2. Beyond Biomarker Response: Multimodality Imaging Evidence Of Cardiac Response After Daratumumab-Based Therapy In AL Amyloidosis

The second AL study prospectively assessed cardiac response after first-line daratumumab, cyclophosphamide, bortezomib, and dexamethasone. Fourteen patients with cardiac AL amyloidosis underwent serial echocardiographic assessment, and 13 had analyzable paired CMR data. Median age was 62.5 years [54.5–69.0], 85.7% were male, and 85.7% had lambda light-chain disease. Renal involvement was present in 42.85%. European modified Mayo stage distribution was stage II in 14.3%, stage IIIA in 71.4%, and stage IIIB in 14.3%.

Results

Baseline NT-proBNP was 3297 ng/L [616.5–4837.5], hs-cTnT was 36.3 ng/L [28.7–76.6], dFLC was 201.5 mg/L [128.5–468], and follow-up occurred after a median of 12.5 months.

Biomarker response was marked. NT-proBNP decreased significantly from 3297 ng/L [616.5–4837.5] at baseline to 669 ng/L [269.5–1612] at follow-up (p=0.001). High-sensitivity troponin T also decreased significantly, from 36.3 ng/L [28.7–76.6] to 29.5 ng/L [19.3–43.4] (p=0.002). Cardiac organ response could be formally assessed in 12 patients with baseline NT-

proBNP ≥650 ng/L, and 10 of these patients (83.3%) met response criteria based on a reduction greater than 30% and greater than 300 ng/L. These results confirmed that daratumumab-based therapy was associated with substantial improvement in myocardial stress and injury biomarkers.

Longitudinal biomarker plots showed paired decreases in NT-proBNP and high-sensitivity cardiac troponin T after treatment, supporting the biomarker response described above.

Serial echocardiography demonstrated partial structural and functional reverse remodeling. Interventricular septal thickness decreased from 15.0 mm [12.5–16.8] to 14.5 mm [13.0–15.0] (p=0.048). Stroke volume index increased from 30.5 to 38.3 mL/m² (p=0.035), suggesting improved forward flow. GLS improved significantly from −10.5% [−17.5 to −9.7] to −13.6% [−17.2 to −10.3] (p=0.038), indicating better longitudinal myocardial deformation. LVEF remained stable, from 55.1% to 56.3% (p=0.245), emphasizing that strain and stroke volume captured improvement not evident from ejection fraction alone.

Diastolic and atrial parameters were less responsive over the relatively short follow-up. Septal and lateral e′ velocities, average E/e′ ratio, and left atrial volume index did not change significantly. Left atrial reservoir strain increased numerically from 10.0% to 19.0%, but this did not reach statistical significance. Right ventricular basal diameter increased slightly, but TAPSE, RV S′, RV free-wall strain, RV global strain, and tricuspid regurgitation velocity remained stable. Overall, the echocardiographic response pattern was characterized by improved wall thickness, GLS, and stroke volume rather than broad normalization of diastolic or right-sided parameters.

Serial CMR provided tissue-level evidence of treatment response. Maximal wall thickness decreased significantly from 17.0 mm [14.0–17.8] to 15.5 mm [12.0–17.5] (p=0.034). Native T1 decreased from 1190 ms [1145–1230] to 1149 ms [1109–1195] (p=0.017), and T2 decreased from 54.0 ms [53.0–55.5] to 51.0 ms [47.0–54.5] (p=0.005). These changes suggest reduced interstitial expansion and myocardial edema or injury. ECV decreased numerically from 49.0% [45.0–56.0] to 47.0% [43.0–53.0], but the difference did not reach statistical significance (p=0.079), likely reflecting limited sample size and technical variability.

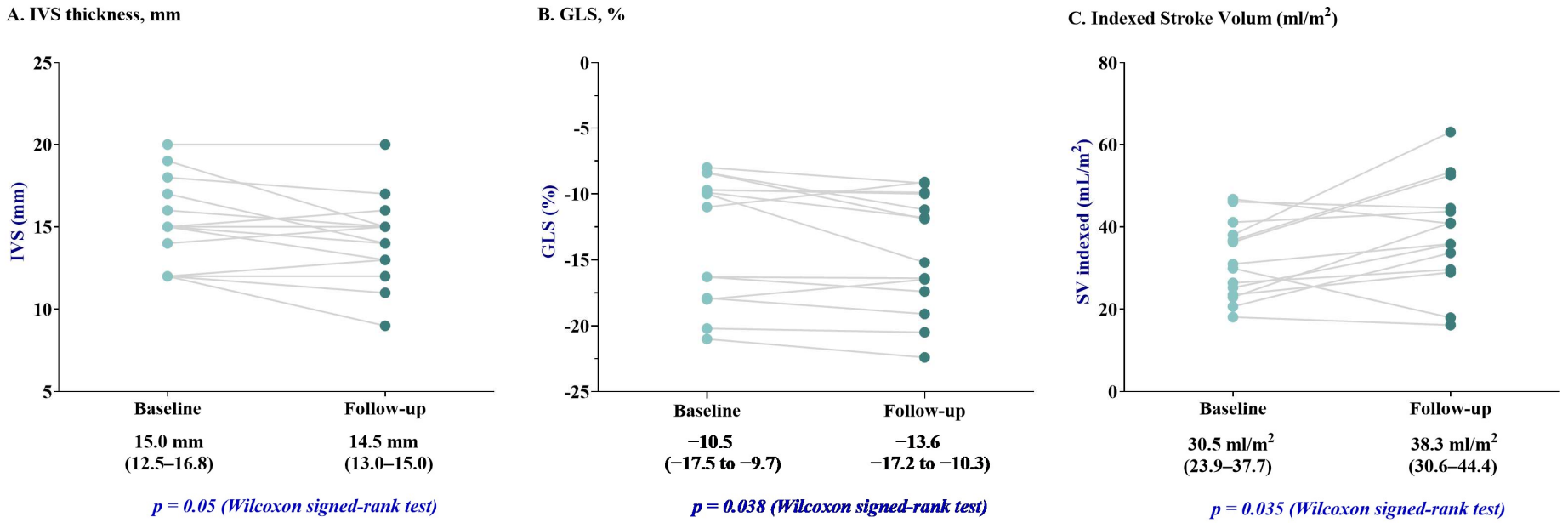


Figure 9. Structural and functional reverse remodeling assessed by serial echocardiography in AL amyloidosis. Paired measurements obtained at baseline and follow-up are shown for interventricular septal thickness (A), left ventricular global longitudinal strain (B), and indexed stroke volume (C). Values are presented as median (interquartile range), and statistical comparisons were performed using the Wilcoxon signed-rank test. Follow-up studies demonstrated significant reductions in wall thickness together with improvements in myocardial deformation and forward stroke volume, supporting the occurrence of partial cardiac reverse remodeling following treatment.

CMR also showed functional and right ventricular remodeling. LVEF improved from 54.1% [52.3–58.8] to 58.1% [52.5–60.4] (p=0.006), while LV mass remained stable. Right ventricular end-diastolic volume index decreased from 69.7 to 62.4 mL/m² (p=0.005), and right ventricular end-systolic volume index decreased from 28.6 to 24.5 mL/m² (p=0.013), while RVEF remained stable. This pattern suggests favorable biventricular remodeling after effective plasma cell-directed therapy.

Table 3. **Cardiac Magnetic Resonance Remodeling Following Treatment**

Parameter	**Baseline**	**Follow-up**	**p-value**
LV EF (%)	**54.1 (52.3–58.8)**	**58.1 (52.5–60.4)**	**0.006**
RV EF (%)	58.1 (51.0–64.5)	55.0 (52.2–62.8)	0.382
Max wall thickness (mm)	**17.0 (14.0–17.8)**	**15.5 (12.0–17.5)**	**0.034**
Native T1 (ms)	**1190 (1145–1230)**	**1149 (1109–1195)**	**0.017**
ECV (%)	49.0 (45.0–56.0)	47.0 (43.0–53.0)	0.079
T2 (ms)	**54.0 (53.0–55.5)**	**51.0 (47.0–54.5)**	**0.005**
LV mass (g/m2)	81.0 (69.0–99.0)	75.0 (66.2–105.5)	0.398
LVEDVi (mL/m²)	78.5 (67.0–91.5)	80.2 (76.2–92.8)	0.055
LVESVi (mL/m²)	34.7 (27.6–46.8)	32.2 (29.6–43.8)	0.279
RVEDVi (mL/m²)	**69.7 (54.3–81.5)**	**62.4 (52.6–80.7)**	**0.005**
RVESVi (mL/m²)	**28.6 (19.7–38.8)**	**24.5 (14.2–34.0)**	**0.013**

Values are presented as median (interquartile range). Comparisons between baseline and follow-up examinations were performed using Wilcoxon signed rank test. . Statistically significant values are shown in bold.

The central result of this study is concordance between biomarker response and imaging-defined myocardial improvement. NT-proBNP and troponin decreased significantly, echocardiography showed improved GLS, stroke volume, and septal thickness, and CMR showed reductions in native T1 and T2, lower maximal wall thickness, improved LVEF, and reverse right ventricular remodeling. Although ECV reduction did not reach statistical

significance, the direction of change was consistent with partial regression of amyloid-related myocardial burden. The study therefore supports the concept that cardiac response in AL amyloidosis should not be assessed only as a biomarker phenomenon. Serial echocardiography and CMR may help identify true myocardial recovery after daratumumab-based therapy and may contribute to future refinements of organ response criteria.

Discussion points

The discussion of the daratumumab-based AL study is framed by the major therapeutic shift introduced by Dara-VCD. The ANDROMEDA trial established daratumumab combined with cyclophosphamide, bortezomib, and dexamethasone as a standard first-line regimen by improving hematologic complete response and organ responses compared with CyBorD alone [78,138]. However, hematologic response and cardiac organ response do not always occur simultaneously, and organ recovery may lag behind clonal control [131,139]. The present study addresses this gap by examining whether deep therapeutic response is accompanied by measurable myocardial remodeling.

Current cardiac response criteria rely mainly on NT-proBNP reduction [133]. More recent graded response criteria suggest that deeper biomarker reductions carry progressively better prognosis and that cardiac response is better conceptualized as a continuum rather than a binary outcome [140,141]. Nevertheless, NT-proBNP is an indirect marker affected by renal function, atrial rhythm, volume status, and supportive therapies. The concordant improvement in biomarkers, echocardiographic deformation, stroke volume, wall thickness, and CMR tissue parameters in this study suggests that multimodality imaging may help distinguish true myocardial recovery from biomarker improvement alone.

The echocardiographic findings are biologically plausible. Improvement in GLS and stroke volume index indicates better longitudinal mechanics and forward flow, while reduction in septal thickness suggests partial structural reverse remodeling. Prior studies have shown that GLS is sensitive to cardiac amyloid burden and can predict outcomes in advanced AL amyloidosis [126]. Because LVEF often remains preserved until late stages, strain and stroke volume may be more responsive markers of early myocardial improvement than ejection fraction alone.

The CMR findings provide the strongest evidence for tissue-level response. Native T1 and ECV quantify interstitial expansion and amyloid burden, while T2 may reflect myocardial edema or injury [12,132]. Previous CMR studies in AL amyloidosis have shown that tissue characterization can guide treatment assessment and that regression of amyloid burden may be

detectable after successful therapy [132]. In the present cohort, significant reductions in native T1 and T2, together with numerical ECV reduction, support the concept of biological myocardial recovery. The lack of statistically significant ECV reduction likely reflects small sample size, technical variability, and the relatively short follow-up.

The study also raises the possibility that future AL response criteria could include imaging-defined cardiac response. Rather than replacing biomarkers, serial echocardiography and CMR may identify patients with true structural and tissue recovery, clarify discordant cases, and help predict long-term outcomes. Larger prospective multicenter cohorts are needed to determine whether reductions in native T1, T2, ECV, wall thickness, or improvements in GLS and stroke volume independently predict survival beyond hematologic and NT-proBNP response.

Limitations include the single-center design, small cohort size, relatively short follow-up, absence of a comparator group, and potential variability in serial CMR quantification. Treatment allocation and supportive therapies were not randomized. Despite these limitations, the prospective design, paired imaging protocol, and concordant direction of biomarker, echocardiographic, and CMR changes strengthen the conclusion that contemporary daratumumab-based therapy may be associated with measurable cardiac reverse remodeling in AL amyloidosis.

Section II Synthesis: Results-Based Contribution

Taken together, the five studies provide a results-driven argument for integrating multimodality imaging into contemporary amyloidosis care. In ATTRv, genotype strongly influenced age at onset, extracardiac phenotype, cardiac involvement, and survival interpretation. In treated hereditary ATTR, a model combining NT-proBNP, eGFR, and GLS outperformed NAC staging and identified three clearly separated risk groups. In treated ATTR cardiomyopathy, serial echocardiography and CMR showed stability of ventricular structure, function, and tissue characterization, supporting stabilization as a meaningful therapeutic endpoint.

In AL amyloidosis, right ventricular dysfunction emerged as a powerful marker of advanced disease severity and enabled identification of a stage IIIC subgroup with median survival of only 2.3 months. After daratumumab-based treatment, biomarker response was accompanied by measurable structural, functional, and tissue-level improvement, suggesting that myocardial recovery can be documented directly with serial imaging. These results support

the thesis conclusion that cardiac amyloidosis should be monitored dynamically, with biomarkers and imaging interpreted together rather than separately.

FINAL CONSIDERATIONS

The thesis demonstrates that cardiac amyloidosis should be approached as a dynamic disease rather than a static infiltrative condition. Modern therapies have changed clinical expectations. In ATTR amyloidosis, disease stabilization is a meaningful therapeutic goal, and serial multimodality imaging can document preservation of cardiac structure, function, and tissue characteristics. In AL amyloidosis, deep hematologic response can translate into measurable myocardial recovery, detectable by echocardiography and CMR.

Across both amyloid subtypes, the thesis supports a broader framework that integrates clinical assessment, biomarkers, and imaging. Biomarkers remain indispensable for diagnosis, staging, and monitoring, but they do not fully describe myocardial structure, function, or tissue composition. Echocardiography provides accessible functional and deformation-based markers, while CMR provides quantitative tissue characterization. Nuclear imaging enables non-invasive ATTR diagnosis and supports subtype differentiation when monoclonal protein is excluded.

The personal contributions of the thesis are clinically relevant in four main ways. First, they describe the distinct phenotype of the Romanian Glu54Gln ATTRv population in comparison with Western European variants. Second, they propose a new staging system for treated hereditary ATTR that combines NT-proBNP, eGFR, and GLS. Third, they show that treated ATTR cardiomyopathy may remain stable on serial echocardiography and CMR. Fourth, they demonstrate that right ventricular dysfunction improves prognostic stratification in AL amyloidosis and that daratumumab-based therapy may be accompanied by imaging evidence of cardiac recovery.

Overall, the thesis argues for a personalized, integrated, and longitudinal model of care in cardiac amyloidosis. Such a model combines early recognition of systemic red flags, accurate subtype diagnosis, risk stratification adapted to contemporary treatment, and repeated multimodality assessment to distinguish progression, stabilization, and recovery. This approach may improve therapeutic timing, patient counseling, follow-up planning, and future development of response criteria.

BIBLIOGRAPHY

1. Rambaran RN, Serpell LC. Amyloid fibrils Abnormal protein assembly. Prion. 2008;2. doi:10.4161/pri.2.3.7488
2. Benson MD, Buxbaum JN, Eisenberg DS, et al. Amyloid nomenclature 2020: update and recommendations by the International Society of Amyloidosis (ISA) nomenclature committee. Amyloid. 2020;27(4):217-222. doi:10.1080/13506129.2020.1835263
3. Garcia-Pavia P, Rapezzi C, Adler Y, et al. Diagnosis and treatment of cardiac amyloidosis: a position statement of the ESC Working Group on Myocardial and Pericardial Diseases. Eur Heart J. 2021;42(16):1554. doi:10.1093/EURHEARTJ/EHAB072
4. Castano A, Narotsky DL, Hamid N, et al. Unveiling transthyretin cardiac amyloidosis and its predictors among elderly patients with severe aortic stenosis undergoing transcatheter aortic valve replacement. Eur Heart J. 2017;38(38):2879-2887. doi:10.1093/EURHEARTJ/EHX350
5. Staron A, Zheng L, Doros G, et al. Marked progress in AL amyloidosis survival: a 40-year longitudinal natural history study. Blood Cancer J. 2021;11(8). doi:10.1038/s41408-021-00529-w
6. Witteles RM, Liedtke M. AL Amyloidosis for the Cardiologist and Oncologist: Epidemiology, Diagnosis, and Management. JACC CardioOncol. 2019;1(1):117-130. doi:10.1016/J.JACCAO.2019.08.002
7. Fontana M, Aimo A, Emdin M, et al. Transthyretin amyloid cardiomyopathy: from cause to novel treatments. Eur Heart J. 2026;47(1):54-63. doi:10.1093/EURHEARTJ/EHAF667
8. Kittleson MM, Maurer MS, Ambardekar AV. Cardiac amyloidosis: evolving diagnosis and management. Circulation. 2020;142(1):e7-e22.
9. Gillmore JD, Damy T, Fontana M, et al. A new staging system for cardiac transthyretin amyloidosis. Eur Heart J. 2018;39(30):2799-2806. doi:10.1093/EURHEARTJ/EHX589
10. Kumar S, Dispenzieri A, Lacy MQ. Revised prognostic staging system for light chain amyloidosis. Journal of Clinical Oncology. 2012;30(9):989-995.
11. Grogan M, Scott CG, Kyle RA, et al. Natural History of Wild-Type Transthyretin Cardiac Amyloidosis and Risk Stratification Using a Novel Staging System. J Am Coll Cardiol. 2016;68(10):1014-1020. doi:10.1016/J.JACC.2016.06.033
12. Fontana M, Chacko LA, Martinez-Naharro A. Detailed Understating of Cardiac Amyloidosis by CMR: Towards Personalized Medicine. JACC Cardiovasc Imaging. 2020;13(6):1311-1313. doi:10.1016/J.JCMG.2020.04.013
13. Gentile L, Diemberger I, Plante-Bordeneuve V, et al. Phenotypic characteristics of F64L, I68L, I107V, and S77Y ATTRv genotypes from the Transthyretin Amyloidosis Outcomes Survey (THAOS). PLoS One. 2024;19(1). doi:10.1371/JOURNAL.PONE.0292435
14. Obi CA, Mostertz WC, Griffin JM, Judge DP. ATTR Epidemiology, Genetics, and Prognostic Factors. Methodist Debakey Cardiovasc J. 2022;18(2):17-26. doi:10.14797/MDCVJ.1066
15. Neculae G, Zaroui A, Kharoubi M, et al. A phenotypic comparison of the Romanian and French ATTRv cohorts: Glu54Gln founder pathogenic variant vs the most common variants in Western Europe. Int J Cardiol. 2025;419. doi:10.1016/J.IJCARD.2024.132714
16. Sanguinetti C, Minniti M, Susini V, et al. The Journey of Human Transthyretin: Synthesis, Structure Stability, and Catabolism. Biomedicines. 2022;10(8). doi:10.3390/BIOMEDICINES10081906
17. Hrncic R, Wall J, Wolfenbarger DA, et al. Antibody-mediated resolution of light chain-associated amyloid deposits. American Journal of Pathology. 2000;157(4):1239-1246. doi:10.1016/S0002-9440(10)64639-1
18. Simon P, Behrens HM, Kristen A, Röcken C. Myocardial inflammatory cells in cardiac amyloidosis. Sci Rep. 2024;14(1). doi:10.1038/S41598-024-74289-5
19. Mazza G, Simons JP, Al-Shawi R, et al. Amyloid persistence in decellularized liver: biochemical and histopathological characterization. Amyloid. 2015;23(1):1. doi:10.3109/13506129.2015.1110518
20. Morfino P, Aimo A, Panichella G, Rapezzi C, Emdin M. Amyloid seeding as a disease mechanism and treatment target in transthyretin cardiac amyloidosis. Heart Fail Rev. 2022;27(6):2187-2200. doi:10.1007/S10741-022-10237-7
21. Yee AW, Aldeghi M, Blakeley MP, et al. A molecular mechanism for transthyretin amyloidogenesis. Nat Commun. 2019;10(1):925. doi:10.1038/s41467-019-08609-z

22. Rajkumar SV. Multiple myeloma: 2022 update on diagnosis, risk stratification, and management. Am J Hematol. 2022;97(8):1086-1107. doi:10.1002/AJH.26590
23. Al Hamed R, Bazarbachi AH, Bazarbachi A, Malard F, Harousseau JL, Mohty M. Comprehensive Review of AL amyloidosis: some practical recommendations. Blood Cancer J. 2021;11(5). doi:10.1038/s41408-021-00486-4
24. Schilling JD, Nuvolone M, Merlini G. The Pathophysiological and Therapeutic Implications of Cardiac Light-Chain Amyloidosis Compared With Transthyretin Amyloidosis. JACC Heart Fail. 2024;12(10):1781-1787. doi:10.1016/J.JCHF.2024.07.003
25. Ueda M, Yamashita T, Misumi Y, Masuda T, Ando Y. Origin of sporadic late-onset hereditary ATTR Val30Met amyloidosis in Japan. Amyloid. 2018;25(3):143-147. doi:10.1080/13506129.2018.1531842
26. Maurer MS, Hanna M, Grogan M, et al. Genotype and Phenotype of Transthyretin Cardiac Amyloidosis: THAOS. J Am Coll Cardiol. 2016;68(2):161-172. doi:10.1016/J.JACC.2016.03.596
27. Jercan A, Ene A, Jurcut R, et al. Clinical characteristics in patients with hereditary amyloidosis with Glu54Gln transthyretin identified in the Romanian population. Orphanet J Rare Dis. 2020;15(1):1-8. doi:10.1186/S13023-020-1309-9
28. Nativi-Nicolau JN, Karam C, Khella S, Mathew M, Maurer S. Screening for ATTR amyloidosis in the clinic: overlapping disorders, misdiagnosis, and multiorgan awareness. Heart Fail Rev. 2021. doi:10.1007/s10741-021-10080-2
29. Rapezzi C, Merlini G, Quarta CC, et al. Systemic cardiac amyloidoses: Disease profiles and clinical courses of the 3 main types. Circulation. 2009;120(13):1203-1212. doi:10.1161/CIRCULATIONAHA.108.843334
30. Brannagan TH, Cheng RK, Clarke JO, et al. 2023 ACC Expert Consensus Decision Pathway on Comprehensive Multidisciplinary Care for the Patient With Cardiac Amyloidosis. J Am Coll Cardiol. 2023. doi:10.1016/J.JACC.2022.11.022
31. Neculae G, Adam R, Jercan A, et al. Cardiac amyloidosis is not a single disease: a multiparametric comparison between the light chain and transthyretin forms. ESC Heart Fail. 2024. doi:10.1002/EHF2.14852
32. Law S, Fontana M, Gillmore JD. Advances in Diagnosis and Treatment of Cardiac and Renal Amyloidosis. Cardiol Clin. 2021;39(3):389-402. doi:10.1016/J.CCL.2021.04.010
33. Kumar S, Dispenzieri A, Lacy MQ, et al. Revised prognostic staging system for light chain amyloidosis incorporating cardiac biomarkers and serum free light chain measurements. J Clin Oncol. 2012;30(9):989-995. doi:10.1200/JCO.2011.38.5724
34. Morioka M, Takashio S, Nakashima N, et al. Correlation Between Cardiac Images, Biomarkers, and Amyloid Load in Wild-Type Transthyretin Amyloid Cardiomyopathy. J Am Heart Assoc. 2022;11(12):24717. doi:10.1161/JAHA.121.024717
35. Feng DL, Edwards WD, Oh JK, et al. Intracardiac thrombosis and embolism in patients with cardiac amyloidosis. Circulation. 2007;116(21):2420-2426. doi:10.1161/CIRCULATIONAHA.107.697763
36. Donnellan E, Elshazly MB, Vakamudi S, et al. No Association Between CHADS-VASc Score and Left Atrial Appendage Thrombus in Patients With Transthyretin Amyloidosis. JACC Clin Electrophysiol. 2019;5(12):1473-1474. doi:10.1016/J.JACEP.2019.10.013
37. Cyrille NB, Goldsmith J, Alvarez J, Maurer MS. Prevalence and Prognostic Significance of Low QRS Voltage Among the Three Main Types of Cardiac Amyloidosis. Am J Cardiol. 2014;114(7):1089-1093. doi:10.1016/J.AMJCARD.2014.07.026
38. Zhao L, Li J, Tian Z, Fang Q. Clinical correlates and prognostic values of pseudoinfarction in cardiac light-chain amyloidosis. J Cardiol. 2016;68(5):426-430. doi:10.1016/J.JJCC.2015.11.004
39. Cappelli F, Vignini E, Martone R, et al. Baseline ECG features and arrhythmic profile in transthyretin versus light chain cardiac amyloidosis. Circ Heart Fail. 2020. doi:10.1161/CIRCHEARTFAILURE.119.006619
40. Jurcut R, Jurcut J, Onciul S, et al. Multimodality imaging in cardiac amyloidosis: a primer for cardiologists. doi:10.1093/ehjci/jeaa063
41. Ando Y, Nakamura M, Araki S. Transthyretin-Related Familial Amyloidotic Polyneuropathy. Arch Neurol. 2005;62(7):1057-1062. doi:10.1001/ARCHNEUR.62.7.1057
42. Adams D, Ando Y, et al. Expert consensus recommendations to improve diagnosis of ATTR amyloidosis with polyneuropathy. J Neurol. 2021;268:2109-2122. doi:10.1007/s00415-019-09688-0
43. England JD, Gronseth GS, Franklin G, et al. Distal symmetrical polyneuropathy: Definition for clinical research. Muscle Nerve. 2005;31(1):113-123. doi:10.1002/MUS.20233

44. Wang AK, Fealey RD, Gehrking TL, Low PA. Patterns of Neuropathy and Autonomic Failure in Patients With Amyloidosis. Mayo Clin Proc. 2008;83(11):1226-1230. doi:10.4065/83.11.1226
45. Adams D, Gonzalez-Duarte A, O'Riordan WD, et al. Patisiran, an RNAi Therapeutic, for Hereditary Transthyretin Amyloidosis. N Engl J Med. 2018;379(1):11-21. doi:10.1056/NEJMOA1716153
46. Benson MD, Waddington-Cruz M, Berk JL, et al. Inotersen Treatment for Patients with Hereditary Transthyretin Amyloidosis. N Engl J Med. 2018;379(1):22-31. doi:10.1056/NEJMOA1716793
47. Dyck PJB, González-Duarte A, Obici L, et al. Development of measures of polyneuropathy impairment in hATTR amyloidosis: From NIS to mNIS+7. J Neurol Sci. 2019;405:116424. doi:10.1016/J.JNS.2019.116424
48. Gastrointestinal Manifestations of Amyloidosis. Am J Gastroenterol. Accessed March 17, 2023.
49. Lim AY, Lee JH, Jung KS, et al. Clinical features and outcomes of systemic amyloidosis with gastrointestinal involvement: a single-center experience. Korean J Intern Med. 2015;30(4):496-505. doi:10.3904/KJIM.2015.30.4.496
50. Sperry BW, Reyes BA, Ikram A, et al. Tenosynovial and Cardiac Amyloidosis in Patients Undergoing Carpal Tunnel Release. J Am Coll Cardiol. 2018;72(17):2040-2050. doi:10.1016/J.JACC.2018.07.092
51. Wang AY, Saini H, Tingen JN, et al. The Relationship Between Wild-Type Transthyretin Amyloid Load and Ligamentum Flavum Thickness in Lumbar Stenosis Patients. World Neurosurg. 2022;164:e113-e118. doi:10.1016/j.wneu.2022.04.008
52. Basdavanos A, Maurer MS, Ives L, et al. Prevalence of Orthopedic Manifestations in Patients With Cardiac Amyloidosis With a Focus on Shoulder Pathologies. Am J Cardiol. 2023;190:67-74. doi:10.1016/j.amjcard.2022.11.014
53. Sueyoshi T, Ueda M, Jono H, et al. Wild-type transthyretin-derived amyloidosis in various ligaments and tendons. Hum Pathol. 2011;42(9):1259-1264. doi:10.1016/J.HUMPATH.2010.11.017
54. Sperry BW, Khedraki R, Gabrovsek A, et al. Cardiac Amyloidosis Screening at Trigger Finger Release Surgery. Am J Cardiol. 2021;160:96-98. doi:10.1016/j.amjcard.2021.08.049
55. Garcia-Pavia P, Bengel F, Brito D, et al. Expert consensus on the monitoring of transthyretin amyloid cardiomyopathy. Eur J Heart Fail. 2021;23(6):895-905. doi:10.1002/EJHF.2198
56. Falk RH, Alexander KM, Liao R, Dorbala S. AL Light-Chain Cardiac Amyloidosis: A Review of Diagnosis and Therapy. J Am Coll Cardiol. 2016;68(12):1323-1341. doi:10.1016/J.JACC.2016.06.053
57. Boldrini M, Cappelli F, Chacko L, et al. Multiparametric Echocardiography Scores for the Diagnosis of Cardiac Amyloidosis. JACC Cardiovasc Imaging. 2020;13(4):909-920. doi:10.1016/J.JCMG.2019.10.011
58. Pan JA, Kerwin MJ, Salerno M. Native T1 Mapping, Extracellular Volume Mapping, and Late Gadolinium Enhancement in Cardiac Amyloidosis: A Meta-Analysis. JACC Cardiovasc Imaging. 2020;13(6):1299-1310. doi:10.1016/J.JCMG.2020.03.010
59. Fontana M, Pica S, Reant P, et al. Prognostic value of late gadolinium enhancement cardiovascular magnetic resonance in cardiac amyloidosis. Circulation. 2015;132(16):1570-1579. doi:10.1161/CIRCULATIONAHA.115.016567
60. Barison A, Aquaro GD, Pugliese NR, et al. Measurement of myocardial amyloid deposition in systemic amyloidosis: insights from cardiovascular magnetic resonance imaging. J Intern Med. 2015;277(5):605-614. doi:10.1111/JOIM.12324
61. Baggiano A, Boldrini M, Martinez-Naharro A, et al. Noncontrast Magnetic Resonance for the Diagnosis of Cardiac Amyloidosis. JACC Cardiovasc Imaging. 2020;13(1):69-80. doi:10.1016/J.JCMG.2019.03.026
62. Karamitsos TD, Papanastasiou CA. Cardiac Magnetic Resonance T1 Mapping for Cardiac Amyloidosis: The Best Way Forward. JACC Cardiovasc Imaging. 2020;13(1):81-82. doi:10.1016/J.JCMG.2019.04.011
63. Dorbala S, Ando Y, Bokhari S, et al. ASNC/AHA/ASE/EANM/HFSA/ISA/SCMR/SNMMI expert consensus recommendations for multimodality imaging in cardiac amyloidosis: Part 2. J Nucl Cardiol. 2019;27(2):659-673. doi:10.1007/S12350-019-01761-5
64. Rubinstein SM, Stockerl-Goldstein K. How to Screen for Monoclonal Gammopathy in Patients With a Suspected Amyloidosis. JACC CardioOncol. 2021;3(4):590-593. doi:10.1016/J.JACCAO.2021.07.001
65. Quarta CC, Gonzalez-Lopez E, Gilbertson JA, et al. Diagnostic sensitivity of abdominal fat aspiration in cardiac amyloidosis. Eur Heart J. 2017;38(24):1905-1908. doi:10.1093/eurheartj/ehx047
66. Wisniowski B, Wechalekar A. Confirming the Diagnosis of Amyloidosis. Acta Haematol. 2020;143(4):312-321. doi:10.1159/000508022

67. Do Amaral B, Coelho T, Sousa A, Guimarães A. Usefulness of labial salivary gland biopsy in familial amyloid polyneuropathy Portuguese type. Amyloid. 2009;16(4):232-238. doi:10.3109/13506120903421850
68. Ruberg FL, Grogan M, Hanna M, Kelly JW, Maurer MS. Transthyretin Amyloid Cardiomyopathy: JACC State-of-the-Art Review. J Am Coll Cardiol. 2019;73(22):2872-2891. doi:10.1016/j.jacc.2019.04.003
69. Hanna M, Ruberg FL, Maurer MS, et al. Cardiac Scintigraphy With Technetium-99m-Labeled Bone-Seeking Tracers for Suspected Amyloidosis. J Am Coll Cardiol. 2020;75(22):2851-2862. doi:10.1016/J.JACC.2020.04.022
70. Gillmore JD, Maurer MS, Falk RH, et al. Nonbiopsy diagnosis of cardiac transthyretin amyloidosis. Circulation. 2016;133(24):2404-2412. doi:10.1161/CIRCULATIONAHA.116.021612
71. Dispenzieri A, Gertz MA, Kyle RA. Serum cardiac troponins and NT-proBNP staging system for AL amyloidosis. J Clin Oncol. 2004;22(18):3751-3757.
72. Wechalekar AD, Schonland SO, Kastritis E, et al. A European collaborative study of treatment outcomes in 346 patients with cardiac stage III AL amyloidosis. Blood. 2013;121(17):3420-3427. doi:10.1182/BLOOD-2012-12-473066
73. Zaroui A, Kharoubi M, Gounot R, et al. Prognostic Mortality Factors in Advanced Light Chain Cardiac Amyloidosis: A Prospective Cohort Study. ESC Heart Fail. 2024;11(3):1707-1719. doi:10.1002/EHF2.14671
74. Khwaja J, Ravichandran S, Bomsztyk J, et al. Limited Utility of Mayo 2012 Cardiac Staging System for Risk Stratification of Patients with Advanced Cardiac AL Amyloidosis. Blood. 2023;142(Suppl 1):537. doi:10.1182/BLOOD-2023-178243
75. Palladini G, Merlini G. How I treat AL amyloidosis. Blood. 2022;139(19):2918-2930. doi:10.1182/BLOOD.2020008737
76. Sanchorawala V, Boccadoro M, Gertz M, et al. Guidelines for high dose chemotherapy and stem cell transplantation for systemic AL amyloidosis. Amyloid. 2022;29(1):1-7. doi:10.1080/13506129.2021.2002841
77. Wechalekar AD, Cibeira MT, Gibbs SD, et al. Guidelines for non-transplant chemotherapy for systemic AL amyloidosis. Amyloid. 2022. doi:10.1080/13506129.2022.2093635
78. Kastritis E, Palladini G, Minnema MC, et al. Daratumumab-Based Treatment for Immunoglobulin Light-Chain Amyloidosis. N Engl J Med. 2021;385(1):46-58. doi:10.1056/NEJMOA2028631
79. Palladini G, Schönland SO, Sanchorawala V, et al. Clarification on the definition of complete haematologic response in light-chain amyloidosis. Amyloid. 2021;28(1):1-2. doi:10.1080/13506129.2020.1868810
80. Griffin JM, Rosenthal JL, Grodin JL, Maurer MS, Grogan M, Cheng RK. ATTR Amyloidosis: Current and Emerging Management Strategies. JACC CardioOncol. 2021;3(4):488-505. doi:10.1016/J.JACCAO.2021.06.006
81. Damy T, Garcia-Pavia P, Hanna M, et al. Efficacy and safety of tafamidis doses in the ATTR-ACT and long-term extension study. Eur J Heart Fail. 2021;23(2):277-285. doi:10.1002/EJHF.2027
82. Berk JL, Suhr OB, Obici L, et al. Repurposing Diflunisal for Familial Amyloid Polyneuropathy: A Randomized Clinical Trial. JAMA. 2013;310(24):2658-2667. doi:10.1001/JAMA.2013.283815
83. Gilad A, Joshi T, Mendelson L, et al. Treating transthyretin amyloid cardiomyopathy: a comparison of diflunisal and tafamidis. J Am Coll Cardiol. 2021;77(18):3296. doi:10.1016/S0735-1097(21)04650-7
84. Penchala SC, Connelly S, Wang Y, et al. AG10 inhibits amyloidogenesis and cellular toxicity of V122I transthyretin. Proc Natl Acad Sci U S A. 2013;110(24):9992-9997. doi:10.1073/PNAS.1300761110
85. Masri A, Aras M, Falk RH, et al. Long-term safety and tolerability of acoramidis in symptomatic transthyretin amyloid cardiomyopathy. J Am Coll Cardiol. 2022;79(9):227. doi:10.1016/S0735-1097(22)01218-9
86. Gillmore JD, Judge DP, Cappelli F, et al. Efficacy and Safety of Acoramidis in Transthyretin Amyloid Cardiomyopathy. N Engl J Med. 2024;390(2):132-142. doi:10.1056/NEJMOA2305434
87. Fontana M, Martinez-Naharro A, Chacko L, et al. Reduction in CMR Derived Extracellular Volume With Patisiran Indicates Cardiac Amyloid Regression. JACC Cardiovasc Imaging. 2021;14(1):189-199. doi:10.1016/J.JCMG.2020.07.043
88. Maurer MS, Fontana M, Berk JL, et al. Primary Results from APOLLO-B, a Phase 3 Study of Patisiran in Patients with Transthyretin-Mediated Amyloidosis with Cardiomyopathy.
89. Maurer MS, Kale P, Fontana M, et al. Patisiran Treatment in Patients with Transthyretin Cardiac Amyloidosis. N Engl J Med. 2023;389(17):1553-1565. doi:10.1056/NEJMOA2300757

90. Fontana M, Berk JL, Gillmore JD, et al. Vutrisiran in Patients with Transthyretin Amyloidosis with Cardiomyopathy. N Engl J Med. 2025;392(1):33-44. doi:10.1056/NEJMOA2409134
91. Adams D, Tournev IL, Taylor MS, et al. Efficacy and safety of vutrisiran for hereditary transthyretin-mediated amyloidosis with polyneuropathy. Amyloid. 2023;30(1). doi:10.1080/13506129.2022.2091985
92. Gillmore JD, Gane E, Taubel J, et al. CRISPR-Cas9 In Vivo Gene Editing for Transthyretin Amyloidosis. N Engl J Med. 2021;385(6):493-502. doi:10.1056/NEJMOA2107454
93. Gillmore JD, Gane E, Täubel J, et al. Nexiguran Ziclumeran Gene Editing in Hereditary ATTR with Polyneuropathy. N Engl J Med. 2025;393(14):1375-1386. doi:10.1056/NEJMOA2510209
94. Khouri MG, Griffin JM. Anti-Fibril Depleters: The Dawn of a New Treatment Era in Transthyretin Amyloid Cardiomyopathy? Circulation. 2026;153(4):226-229. doi:10.1161/CIRCULATIONAHA.125.078276
95. Suhr OB, Grogan M, Silva AM da, et al. PRX004 in variant ATTRv amyloidosis: phase 1 study. Amyloid. 2025;32(1):14-21. doi:10.1080/13506129.2024.2420809
96. Bodin K, Ellmerich S, Kahan MC, et al. Antibodies to human serum amyloid P component eliminate visceral amyloid deposits. Nature. 2010;468(7320):93-97. doi:10.1038/nature09494
97. Cheng RK, Levy WC, Vasbinder A, et al. Diuretic Dose and NYHA Functional Class Are Independent Predictors of Mortality in Transthyretin Cardiac Amyloidosis. JACC CardioOncol. 2020;2(3):414-424. doi:10.1016/J.JACCAO.2020.06.007
98. Aimo A, Vergaro G, Castiglione V, Rapezzi C, Emdin M. Safety and Tolerability of Neurohormonal Antagonism in Cardiac Amyloidosis. Eur J Intern Med. 2020;80:66-72. doi:10.1016/J.EJIM.2020.05.015
99. Barge-Caballero G, Barge-Caballero E, López-Pérez M, et al. Beta-Blocker Exposure and Survival in Transthyretin Amyloid Cardiomyopathy. Mayo Clin Proc. 2022;97(2):261-273. doi:10.1016/j.mayocp.2021.08.006
100. Palma JA, Gonzalez-Duarte A, Kaufmann H. Orthostatic hypotension in hereditary transthyretin amyloidosis. Clin Auton Res. 2019;29(1):33-44. doi:10.1007/S10286-019-00623-X
101. Anker SD, Butler J, Filippatos G, et al. Empagliflozin in Heart Failure with a Preserved Ejection Fraction. N Engl J Med. 2021;385(16):1451-1461. doi:10.1056/NEJMOA2107038
102. Porcari A, Cappelli F, Nitsche C, et al. SGLT2 Inhibitor Therapy in Patients With Transthyretin Amyloid Cardiomyopathy. J Am Coll Cardiol. 2024;83(24):2411-2422. doi:10.1016/J.JACC.2024.03.429
103. Lang FM, Teruya S, Cuomo M, et al. Safety and Efficacy of SGLT2 Inhibitors for Amyloid Light-Chain Cardiomyopathy. J Card Fail. 2024;30(12):1641-1646. doi:10.1016/j.cardfail.2024.06.009
104. Feng DL, Syed IS, Martinez M, et al. Intracardiac Thrombosis and Anticoagulation Therapy in Cardiac Amyloidosis. Circulation. 2009;119(18):2490-2497. doi:10.1161/CIRCULATIONAHA.108.785014
105. Pollak A, Falk RH. Left ventricular systolic dysfunction precipitated by verapamil in cardiac amyloidosis. Chest. 1993;104(2):618-620. doi:10.1378/CHEST.104.2.618
106. Mints YY, Doros G, Berk JL, Connors LH, Ruberg FL. Features of atrial fibrillation in wild-type transthyretin cardiac amyloidosis. ESC Heart Fail. 2018;5(5):772-779. doi:10.1002/EHF2.12308
107. El-Am EA, Dispenzieri A, Melduni RM, et al. Direct Current Cardioversion of Atrial Arrhythmias in Cardiac Amyloidosis. J Am Coll Cardiol. 2019;73(5):589-597. doi:10.1016/J.JACC.2018.10.079
108. Black-Maier E, Rehorn M, Loungani R, et al. Catheter ablation of atrial fibrillation in cardiac amyloidosis. PACE. 2020;43(9):913-921. doi:10.1111/PACE.13992
109. Zeppenfeld K, Tfelt-Hansen J, De Riva M, et al. 2022 ESC Guidelines for ventricular arrhythmias and sudden cardiac death prevention. Eur Heart J. 2022;43(40):3997-4126. doi:10.1093/EURHEARTJ/EHAC262
110. Algalarrondo V, Dinanian S, Juin C, et al. Prophylactic pacemaker implantation in familial amyloid polyneuropathy. Heart Rhythm. 2012;9(7):1069-1075. doi:10.1016/J.HRTHM.2012.02.033
111. Mehra MR, Canter CE, Hannan MM, et al. The 2016 International Society for Heart Lung Transplantation listing criteria for heart transplantation. J Heart Lung Transplant. 2016;35(1):1-23. doi:10.1016/J.HEALUN.2015.10.023
112. Griffin JM, Baughan E, Rosenblum H, et al. Surveillance for disease progression of transthyretin amyloidosis after heart transplantation. J Heart Lung Transplant. 2022;41(2):199-207. doi:10.1016/J.HEALUN.2021.10.007
113. Michelis KC, Zhong L, Tang WHW, et al. Durable Mechanical Circulatory Support in Amyloid Cardiomyopathy: Insights From INTERMACS. Circ Heart Fail. 2020;13(12):E007931. doi:10.1161/CIRCHEARTFAILURE.120.007931

114. Damy T, Kristen AV, Suhr OB, et al. Transthyretin cardiac amyloidosis in continental Western Europe: THAOS. Eur Heart J. doi:10.1093/eurheartj/ehz173
115. Gentile L, Coelho T, Dispenzieri A, et al. A 15-year consolidated overview of data in over 6000 patients from THAOS. Orphanet J Rare Dis. 2023;18(1). doi:10.1186/S13023-023-02962-5
116. Waddington-Cruz J, Wixner J, Amass L, Kiszko J, Chapman D. Characteristics of Patients with Late- vs. Early-Onset Val30Met Transthyretin Amyloidosis from THAOS. Neurol Ther. doi:10.1007/s40120-021-00258-z
117. Neculae G, Adam R, Beyer R, et al. Novel transthyretin variant linked to cardiac amyloidosis in the Romanian population. Arch Cardiovasc Dis. 2024;117(1):S38-S39. doi:10.1016/J.ACVD.2023.10.068
118. Damy T, Zaroui A, de Tournemire M, et al. Changes in amyloidosis phenotype over 11 years in a cardiac amyloidosis referral centre cohort in France. Arch Cardiovasc Dis. 2023;116(10):433-446. doi:10.1016/J.ACVD.2023.07.003
119. Conceição I, Damy T, Romero M, et al. Early diagnosis of ATTR amyloidosis through targeted follow-up of TTR mutation carriers. Amyloid. 2019;26(1):3-9. doi:10.1080/13506129.2018.1556156
120. Damy T, Bourel G, Slama M, et al. Incidence and survival of transthyretin amyloid cardiomyopathy from a French nationwide study. Orphanet J Rare Dis. 2023;18:345. doi:10.1186/s13023-023-02933-w
121. Maurer MS, Grogan DR, Judge DP, et al. Tafamidis in Transthyretin Amyloid Cardiomyopathy: Effects on Transthyretin Stabilization and Clinical Outcomes. Circ Heart Fail. 2015;8(3):519-526. doi:10.1161/CIRCHEARTFAILURE.113.000890
122. Garcia-Pavia P, Kristen AV, Drachman B, et al. Survival in a Real-World Cohort of Patients With Transthyretin Amyloid Cardiomyopathy Treated With Tafamidis: THAOS. J Card Fail. 2024. doi:10.1016/J.CARDFAIL.2024.06.003
123. Maurer MS, Schwartz JH, Gundapaneni B, et al. Tafamidis Treatment for Patients with Transthyretin Amyloid Cardiomyopathy. N Engl J Med. 2018;379(11):1007-1016. doi:10.1056/NEJMOA1805689
124. Fontana M, Berk JL, Gillmore JD, et al. Vutrisiran in Patients with Transthyretin Amyloidosis with Cardiomyopathy. N Engl J Med. 2024. doi:10.1056/NEJMOA2409134
125. Giblin GT, Cuddy SAM, González-López E, et al. Effect of tafamidis on global longitudinal strain and myocardial work in transthyretin cardiac amyloidosis. Eur Heart J Cardiovasc Imaging. 2022;23(8):1029. doi:10.1093/EHJCI/JEAC049
126. Lee Chuy K, Drill E, Yang JC, et al. Incremental Value of Global Longitudinal Strain for Predicting Survival in Advanced AL Amyloidosis. JACC CardioOncol. 2020;2(2):223. doi:10.1016/J.JACCAO.2020.05.012
127. Witteles R, Jefferies JL, Kapa S, et al. Atrial Fibrillation as a Prognostic Factor for All-Cause Mortality in Transthyretin Amyloid Cardiomyopathy. JACC CardioOncol. 2024;6(4):592-598. doi:10.1016/J.JACCAO.2024.03.007
128. Barroso FA, Coelho T, Dispenzieri A, et al. Characteristics of patients with autonomic dysfunction in THAOS. Amyloid. 2022;29(3):175-183. doi:10.1080/13506129.2022.2043270
129. Patel R, Martinez-Naharro A, Razvi Y, et al. Cardiovascular Magnetic Resonance in Transthyretin Amyloid Cardiomyopathy: natural history and treatment response. J Cardiovasc Magn Reson. 2024;26:100356. doi:10.1016/j.jocmr.2024.100356
130. Martinez-Naharro A, Kotecha T, Norrington K, et al. Native T1 and Extracellular Volume in Transthyretin Amyloidosis. JACC Cardiovasc Imaging. 2019;12(5):810-819. doi:10.1016/j.jcmg.2018.02.006
131. Sidana S, Milani P, Binder M, et al. A validated composite organ and hematologic response model for early assessment of treatment outcomes in light chain amyloidosis. Blood Cancer J. 2020;10(4):41. doi:10.1038/s41408-020-0306-5
132. Martinez-Naharro A, Patel R, Kotecha T, et al. Cardiovascular magnetic resonance in light-chain amyloidosis to guide treatment. Eur Heart J. 2022;43(45):4722-4735. doi:10.1093/EURHEARTJ/EHAC363
133. Palladini G, Dispenzieri A, Gertz MA, et al. Validation of the Criteria of Response to Treatment in AL Amyloidosis. Blood. 2010;116(21):1364. doi:10.1182/BLOOD.V116.21.1364.1364
134. Tjahjadi C, Fortuni F, Stassen J, et al. Prognostic Implications of Right Ventricular Systolic Dysfunction in Cardiac Amyloidosis. Am J Cardiol. 2022;173:120-127. doi:10.1016/j.amjcard.2022.02.048
135. Ghio S, Perlini S, Palladini G, et al. Importance of the Echocardiographic Evaluation of Right Ventricular Function in AL Amyloidosis. Eur J Heart Fail. 2007;9(8):808-813. doi:10.1016/J.EJHEART.2007.05.006

136. Cappelli F, Porciani MC, Bergesio F, et al. Right ventricular function in AL amyloidosis: characteristics and prognostic implication. Eur Heart J Cardiovasc Imaging. 2012;13(5):416-422. doi:10.1093/EJECHOCARD/JER289
137. Tomasoni D, Adamo M, Porcari A, et al. Right ventricular to pulmonary artery coupling and outcome in cardiac amyloidosis. Eur Heart J Cardiovasc Imaging. 2023;24(10):1405-1414. doi:10.1093/EHJCI/JEAD145
138. Kastritis E, Palladini G, Minnema MC. Daratumumab-based treatment for AL amyloidosis. N Engl J Med. 2021;385(1):46-58.
139. Gertz MA, Comenzo R, Falk RH, et al. Definition of organ involvement and treatment response in immunoglobulin light chain amyloidosis: consensus opinion. Am J Hematol. 2005;79:319-328. doi:10.1002/ajh.20381
140. Muchtar E, Dispenzieri A, Wisniowski B, et al. Graded Cardiac Response Criteria for Systemic Light Chain Amyloidosis. J Clin Oncol. 2023;41(7):1393-1403. doi:10.1200/JCO.22.00643
141. Muchtar E, Geyer S, Merlini G, Gertz MA. Patients with a cardiac complete response in AL amyloidosis have survival rates similar to those of a matched general population. Blood. 2024;144(7):790-793. doi:10.1182/BLOOD.2024024623